



ELSEVIER

Contents lists available at SciVerse ScienceDirect

Journal of Differential Equations

www.elsevier.com/locate/jde



Heteroclinic tangles in time-periodic equations

Fengjuan Chen^{a,*,1}, Ali Oksasoglu^b, Qiu Dong Wang^{c,*,2}^a Department of Mathematics, Zhejiang Normal University, Jinhua, Zhejiang 321004, PR China^b Honeywell Corporation, 11100 N. Oracle Rd., Tucson, AZ 85737, USA^c Department of Mathematics, University of Arizona, Tucson, AZ 85721, USA

ARTICLE INFO

Article history:

Received 9 July 2012

Available online 31 October 2012

MSC:

37D45

37C40

Keywords:

Time-periodic differential equations

Chaotic dynamics

Heteroclinic tangles

Separatrix maps

ABSTRACT

In this paper we prove that, when a heteroclinic loop is periodically perturbed, *three* types of heteroclinic tangles are created and they compete in the space of μ where μ is a parameter representing the magnitude of the perturbations. The three types are (a) transient heteroclinic tangles containing no Gibbs measures; (b) heteroclinic tangles dominated by sinks representing stable dynamical behavior; and (c) heteroclinic tangles with strange attractors admitting SRB measures representing chaos. We also prove that, as $\mu \rightarrow 0$, the organization of the three types of heteroclinic tangles depends sensitively on the ratio of the unstable eigenvalues of the saddle fixed points of the heteroclinic connections. The theory developed in this paper is explicitly applicable to the analysis of various specific differential equations and the results obtained are well beyond the capacity of the classical Birkhoff–Melnikov–Smale method.

© 2012 Elsevier Inc. All rights reserved.

1. Introduction

Modern chaos theory was originated from the discovery of homoclinic tangles by Henry Poincaré in his study of periodically forced ordinary differential equations [18]. When a homoclinic solution of an autonomous differential equation is periodically perturbed, the stable and unstable manifold of the perturbed saddle would intersect, creating homoclinic tangles hence exceedingly complicated dynamics [7,24,25]. One of the most celebrated achievements of the modern chaos theory is the

* Corresponding authors.

E-mail addresses: fjchen@zjnu.cn (F. Chen), ali.oksasoglu@honeywell.com (A. Oksasoglu), dwang@math.arizona.edu (Q. Wang).

¹ Fengjuan Chen is partially supported by Zhejiang Innovation Project Grant NO:T200905.² Qiu Dong Wang is partially supported by a NSF grant.

construction of the Smale horseshoe in all homoclinic tangles and the establishment of the Birkhoff–Smale–Melnikov method, by which the theory of horseshoes can be applied to the analysis of various specific systems of differential equations [1,5,11,10,13,22,23].

There have remained, however, many unanswered questions about the dynamics of homoclinic tangles. Here we list three. The first question is on the gap in between the theory of horseshoes and the numerous pictures of chaos generated in numerical and lab simulations [26,12,6,8]. Dynamic structures revealed by direct simulations of solution are likely those with an attractive basin of positive Lebesgue measure in phase space. But the attractive basin of the Smale horseshoe is of Lebesgue measure zero. Therefore, in addressing pictures of chaos obtained by direct simulations of solutions, the relevancy of horseshoes obtained by Birkhoff–Smale–Melnikov method was never clearly established. The second question is about the lacking of a comprehensive understanding of the overall structure of homoclinic tangles. In a homoclinic tangle, horseshoes are only one participating part. A homoclinic tangle might also contain other dynamical objects, such as Newhouse sinks and strange attractors with SRB measures [16,21,20,3]. Here the question is to mathematically identify various participating parts and to understand the way they fit together in homoclinic tangles. The third question is on applications. Profound dynamics theories on non-uniformly hyperbolic maps, such as the theory of SRB measures, the theory of Newhouse tangency, and the theory of rank one chaos, have been introduced in the last thirty years [9,19,17,2,4,15,30–33]. These theories are all directly related to the study of homoclinic tangles. But to apply them to the analysis of specific maps, let alone that of specific differential equations, has been mathematically challenging. As far as the issue of analysis of various specific differential equations is concerned, there has existed no parallel of Birkhoff–Smale–Melnikov method for these new theories to apply.

In a sequence of recently papers [27–29], Wang and his coauthors have answered these three questions for certain homoclinic tangles in periodically perturbed equations with homoclinic solutions to a dissipative saddle. The study of [27] revealed that there exist *three kind* of homoclinic tangles, the occurrence of each depends sensitively on the magnitude of the periodic forcing. As far as directly observable dynamical objects, that is, those with an attractive basin of positive Lebesgue measure, are concerned, the three kind of homoclinic tangles are (a) transient tangles, (b) stable tangles, and (c) chaotic tangles. A transient tangle contains no directly observable dynamical object; a stable tangle contains only asymptotically stable periodic solutions (as directly observable objects); and chaotic tangles contain strange attractors with SRB measures. They also found that, as the forcing magnitude approaches to zero, the occurrence of these three kind of homoclinic tangles are regulated by a fixed pattern, repeating infinitely many times in an accelerated fashion. Note that the Smale horseshoe is contained in all three kind but horseshoes are not relevant in this description because they are not directly observable object. In [28], the predictions of this new theory are tested through numerical simulation of a specific equation. Numerical integrations always produced one of the three kind of homoclinic tangles of the theory, and the fixed pattern of their repeated occurrence in the space of perturbation parameter, as predicted by the theory, lasted down to $\mu = 10^{-8}$ where μ is the magnitude of the perturbation. This is the first time a theory on the dynamics of periodically perturbed homoclinic solutions has matched the results of numerical simulations systematically in perfection. In [29], the authors proved that, when stable and unstable manifolds of the perturbed saddle point are completely pulled apart by periodic perturbation, a case Birkhoff–Smale–Melnikov fails to apply, there remain horseshoes and chaotic rank one attractors of [30] provided that the forcing frequency is sufficiently large. These study revealed that, when a homoclinic solution is periodically perturbed, expansions in phase space are induced by two vary different mechanisms. The first is a logarithmic singularity associated to transversal homoclinic intersection, responsible for the Smale horseshoe. The second is a regular non-uniform expansion associated to large forcing frequency, responsible for directly observable dynamical objects of complicated structure.

The main purpose of this paper is to extend the theory of [27,28] for homoclinic tangles to the study of heteroclinic tangles. This is to say that we aim at developing a *comprehensive theory* on the dynamics of heteroclinic tangles that are *directly applicable* to the analysis of various specific differential equations. We prove that, when a heteroclinic loop is periodically perturbed, *three* types of heteroclinic tangles are created and they compete in the space of μ where μ is a parameter representing the magnitude of the perturbation. The three types are (a) transient heteroclinic tan-

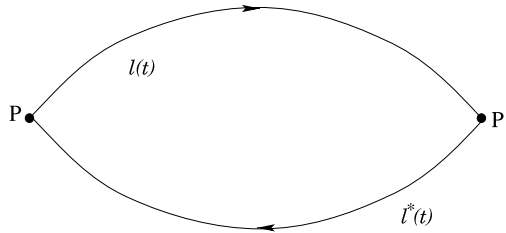


Fig. 1. Heteroclinic loop of the unforced equation.

gles containing no Gibbs measures; (b) heteroclinic tangles dominated by sinks representing stable dynamical behavior; and (c) heteroclinic tangles with strange attractors admitting SRB measures representing chaos. We also prove that, as $\mu \rightarrow 0$, the organization of the three types of heteroclinic tangles depends sensitively on the ratio of the unstable eigenvalues of the saddle fixed points of the heteroclinic connections. If the two unstable eigenvalues, which we denote as β and β^* , are rationally related, say, $\beta/\beta^* = m/n$ where m, n are integers, then the occurrence of the three types of heteroclinic tangles form a pattern that repeats infinitely many times in an accelerated fashion as $\mu \rightarrow 0$, and the *multiplicative period* in μ is $e^{\beta n T} = e^{\beta^* m T}$ where T is the forcing period. As the order of the resonance of β and β^* goes higher, the multiplicative period gets larger and the repeating periodic pattern becomes more complicated. The periodicity of dynamical behavior in μ would disappear as β and β^* become irrationally related.

It is critically important that a method developed for differential equations can be applied to various specific equations. It is equally important for us to illustrate that the results of our theory systematically match the results of numerical simulations. The dynamics theory, developed in Sections 2–4 of this paper, is indeed explicitly applicable to the analysis of various specific differential equations with either a heteroclinic or a homoclinic loop forced by a general periodic perturbation. A comprehensive scheme motivated by this new dynamics theory is also introduced for the numerical explorations of the dynamics of heteroclinic tangles. Systematic applications of both the theory and the numerical scheme to a given example are worked out in detail in Section 5, which is an integral part of this paper.

2. Statement of results

2.1. Equations of study

Let $(x, y) \in \mathbb{R}^2$ be the phase variables and t be the time. We start with the following autonomous differential equations:

$$\frac{dx}{dt} = f(x, y), \quad \frac{dy}{dt} = g(x, y) \quad (2.1)$$

where $f(x, y), g(x, y)$ are analytic functions defined on an open domain $\mathbf{V} \subset \mathbb{R}^2$. We assume that Eq. (2.1) has two saddle fixed points in \mathbf{V} , which we denote as $P = (q, p)$, $P^* = (q^*, p^*)$. Let $\alpha < 0 < \beta$ be the eigenvalues of the Jacobian matrix of (2.1) at P , and ξ_α, ξ_β be their respective eigenvectors. Let $\alpha^* < 0 < \beta^*$, $\xi_{\alpha^*}, \xi_{\beta^*}$ be the corresponding eigenvalues and eigenvectors for P^* . We assume that both P and P^* are *dissipative* and *non-resonant*. This is to assume

(H1) $|\alpha| > \beta, |\alpha^*| > \beta^*$. In addition, α is not rationally related to β , and α^* is not rationally related to β^* .

We also assume that (2.1) has two heteroclinic solutions in \mathbf{V} : One from P to P^* , which we denote as $\ell = \{\ell(t) = (a(t), b(t)), t \in \mathbb{R}\}$; and the other from P^* to P , which we denote as $\ell^* = \{\ell^*(t) = (a^*(t), b^*(t)), t \in \mathbb{R}\}$. This is shown in Fig. 1.

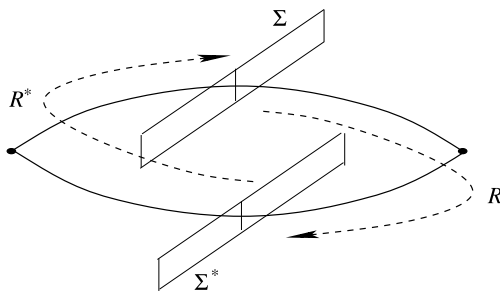


Fig. 2. The separatrix map $\mathcal{F} = \mathcal{R}^* \circ \mathcal{R}$.

To the right of Eq. (2.1) we add a forcing term to form a non-autonomous equation

$$\frac{dx}{dt} = f(x, y) + \mu P(x, y, t), \quad \frac{dy}{dt} = g(x, y) + \mu Q(x, y, t) \quad (2.2)$$

where μ is a small parameter and $P(x, y, t), Q(x, y, t) : \mathbf{V} \times \mathbb{R} \rightarrow \mathbb{R}$ are C^∞ . We assume that $P(x, y, t), Q(x, y, t)$ are periodic in t and are high order terms at $(x, y) = (q, p)$ and (q^*, p^*) . This is to assume

(H2) $P(x, y, t), Q(x, y, t) : \mathbf{V} \times \mathbb{R} \rightarrow \mathbb{R}$ are C^∞ and they are such that

- (i) $P(x, y, t + T) = P(x, y, t), Q(x, y, t + T) = Q(x, y, t)$ where $T > 0$ is a constant;
- (ii) the value of $P(x, y, t), Q(x, y, t)$ and their first derivatives with respect to x and y are all zero at $(x, y) = (q, p)$ and (q^*, p^*) for all t .

We introduce an angular variable $\theta \in S^1 := \mathbb{R}/\{nT\}$ to rewrite Eq. (2.2) as

$$\frac{dx}{dt} = f(x, y) + \mu P(x, y, \theta), \quad \frac{dy}{dt} = g(x, y) + \mu Q(x, y, \theta), \quad \frac{d\theta}{dt} = 1. \quad (2.3)$$

We study the solutions of Eq. (2.3) around the heteroclinic loop $\ell \cup \ell^*$ in the extended phase space (x, y, θ) on $\mathbf{V} \times S^1$. In the (x, y) -plane, let σ, σ^* be two short segments, transversally intersecting ℓ and ℓ^* respectively. Let $\Sigma = \sigma \times S^1, \Sigma^* = \sigma^* \times S^1$ be their respective correspondence in the extended phase space. Let \mathcal{R}_μ be the map induced by the solutions of Eq. (2.3) from Σ to Σ^* ; and \mathcal{R}_μ^* from Σ^* to Σ . This is shown in Fig. 2. The return map $\mathcal{F}_\mu = \mathcal{R}_\mu^* \circ \mathcal{R}_\mu : \Sigma \rightarrow \Sigma$ is the *separatrix map* around $\ell \cup \ell^*$. Denote

$$\Omega_\mu := \{(x, y, \theta) \in \Sigma : \mathcal{F}_\mu^n(x, y, \theta) \in \Sigma, \forall n \in \mathbb{Z}^+\}$$

and let

$$\Lambda_\mu = \bigcap_{n \in \mathbb{Z}^+} \mathcal{F}_\mu^n(\Omega_\mu).$$

The set Ω_μ represents all solutions of Eq. (2.3) that stay around the unforced heteroclinic loop in forward time and Λ_μ represents all solutions that stay around the heteroclinic loop for all time. The set Λ_μ is the *heteroclinic tangle*, the geometrical and dynamical structure of which we study in this paper.

2.2. Statement of theorems

We start with the Melnikov functions $\mathcal{W}(\theta)$ and $\mathcal{W}^*(\theta)$, explicitly defined for the unperturbed heteroclinic solutions ℓ and ℓ^* respectively. Let

$$\tau_\ell(t) = \frac{1}{|\ell'(t)|} \ell'(t), \quad \tau_{\ell^*}(t) = \frac{1}{|(\ell^*)'(t)|} (\ell^*)'(t)$$

be the unit tangent vectors of the heteroclinic solutions at $\ell(t)$ and $\ell^*(t)$ respectively. We have

$$\begin{aligned} \lim_{t \rightarrow -\infty} \tau_\ell(t) &= \xi_\beta, & \lim_{t \rightarrow +\infty} \tau_\ell(t) &= -\xi_{\alpha^*}; \\ \lim_{t \rightarrow -\infty} \tau_{\ell^*}(t) &= \xi_{\beta^*}, & \lim_{t \rightarrow +\infty} \tau_{\ell^*}(t) &= -\xi_\alpha. \end{aligned}$$

We also use $\tau_\ell^\perp(t)$ to denote a unit vector that is perpendicular to $\tau_\ell(t)$ (for $\tau = (u, v)$, $\tau^\perp = (v, -u)$) and $\tilde{\tau}_\ell^\perp(t)$ its transpose. Let

$$\mathcal{W}(\theta) = \int_{-\infty}^{\infty} \left[(P(\ell(t), t + \theta), Q(\ell(t), t + \theta)) \cdot \tau_{\ell(t)}^\perp \right] e^{-\int_0^t E_\ell(s) ds} dt \quad (2.4)$$

where

$$E_\ell(t) = \tau_{\ell(t)}^\perp \begin{pmatrix} \partial_x f(\ell(t)) & \partial_y f(\ell(t)) \\ \partial_x g(\ell(t)) & \partial_y g(\ell(t)) \end{pmatrix} \tilde{\tau}_{\ell(t)}^\perp. \quad (2.5)$$

One can verify that

$$\lim_{t \rightarrow +\infty} E_\ell(t) = \beta^*, \quad \lim_{t \rightarrow -\infty} E_\ell(t) = \alpha,$$

from which it follows that $\mathcal{W}(\theta)$ is well-defined. Similarly, we let

$$\mathcal{W}^*(\theta) = \int_{-\infty}^{\infty} \left[(P(\ell^*(t), t + \theta), Q(\ell^*(t), t + \theta)) \cdot \tau_{\ell^*(t)}^\perp \right] e^{-\int_0^t E_{\ell^*}(s) ds} dt \quad (2.6)$$

where

$$E_{\ell^*}(t) = \tau_{\ell^*(t)}^\perp \begin{pmatrix} \partial_x f(\ell^*(t)) & \partial_y f(\ell^*(t)) \\ \partial_x g(\ell^*(t)) & \partial_y g(\ell^*(t)) \end{pmatrix} \tilde{\tau}_{\ell^*(t)}^\perp. \quad (2.7)$$

The function $\mathcal{W}^*(\theta)$ is also well-defined because

$$\lim_{t \rightarrow +\infty} E_{\ell^*}(t) = \beta, \quad \lim_{t \rightarrow -\infty} E_{\ell^*}(t) = \alpha^*.$$

We also assume

(H3) $\mathcal{W}(\theta)$ and $\mathcal{W}^*(\theta)$ are such that,

- (i) $\min_{\theta \in S^1} \mathcal{W}(\theta), \min_{\theta \in S^1} \mathcal{W}^*(\theta) < 0 < \max_{\theta \in S^1} \mathcal{W}(\theta), \max_{\theta \in S^1} \mathcal{W}^*(\theta)$;
- (ii) if $\mathcal{W}(\theta_0) = 0$, then $\mathcal{W}'(\theta_0) \neq 0$; and if $\mathcal{W}^*(\theta_0) = 0$, then $(\mathcal{W}^*)'(\theta_0) \neq 0$.

Standing assumptions. In the rest of this paper we assume (H1)–(H3).

Theorem 2.1 (Birkhoff–Melnikov–Smale). *There exists a $\mu_0 > 0$ such that for all $0 < \mu < \mu_0$, the heteroclinic tangle Λ_μ contains a horseshoe of infinitely many branches.*

This theorem is a version of the classical Birkhoff–Melnikov–Smale. We also have

Theorem 2.2 (Sinks of strong contraction). *There exist infinitely many disjoint open intervals $\{\tilde{I}_n\}$ of μ approaching $\mu = 0$, such that for all $\mu \in \bigcup_n \tilde{I}_n$, Λ_μ admits a periodic sink.*

As we will see from the proof of Theorem 2.2, the sinks of Theorem 2.2 are *not* the classical Newhouse sinks associated with the phenomenon of transversal homoclinic and heteroclinic tangency. The sinks of Theorem 2.2 tend to be more dominating in the sense that they are strongly contractive. In comparison, the Newhouse sinks have much weaker contractions and much longer periods.

It turns out that the Newhouse tangency is also a major dynamical scenario, as asserted by the next theorem. Denote

$$C = \lim_{t \rightarrow -\infty} \frac{1}{\beta} \ln e^{-\beta t} |\ell(t) - P|, \quad C^* = \lim_{t \rightarrow -\infty} \frac{1}{\beta^*} \ln e^{-\beta^* t} |\ell^*(t) - P^*| \quad (2.8)$$

and let

$$I_+ = \{\theta \in [0, T): \mathcal{W}(\theta - C) > 0\}, \quad I_- = \{\theta \in [0, T): \mathcal{W}(\theta - C) < 0\}; \quad (2.9)$$

I_+^*, I_-^* are similarly defined by using $\mathcal{W}^*(\theta - C^*)$. We define the dynamical functions $\mathcal{D}(\theta)$ and $\mathcal{D}^*(\theta)$ by letting

$$\mathcal{D}(\theta) = \theta - \frac{1}{\beta^*} \ln \mathcal{W}(\theta - C); \quad \mathcal{D}^*(\theta) = \theta - \frac{1}{\beta} \ln \mathcal{W}^*(\theta - C^*). \quad (2.10)$$

Let \mathcal{C} be the set of critical points of $\mathcal{D}(\theta)$ in I_+ and \mathcal{C}^* the set of critical points of $\mathcal{D}^*(\theta)$ in I_+^* .

Theorem 2.3. *Assume that there exists a non-degenerate critical point either for $\mathcal{D}(\theta)$ in \mathcal{C} or for $\mathcal{D}^*(\theta)$ in \mathcal{C}^* . Then there exists a sequence $\mu_n \rightarrow 0$, such that for every n , and $\hat{\mu} = \mu_n$,*

- (a) (Newhouse sinks) *there exists $\hat{\mu}_k \rightarrow \hat{\mu}$, such that $\Lambda_{\hat{\mu}_k}$ for $\hat{\mu}_k$ admits periodic sinks;*
- (b) (Strange attractors) *there exists a set of positive Lebesgue measure of μ close to $\hat{\mu}$, such that the corresponding heteroclinic tangle Λ_μ admits strange attractors with an SRB measure.*

Theorem 2.3 provides a way of applying the Newhouse theory, the theory of Hénon-like maps and the theory of SRB measures to a given set of differential equations. Both the sinks and the SRB measures of Theorem 2.3 are associated with transversal homoclinic tangency. The periodic sinks asserted in Theorem 2.3(a) are Newhouse sinks, and the strange attractors of Theorem 2.3(b) are Hénon-like attractors.

We need a few more quantities to state our next theorem. Denote

$$\begin{aligned} \mathcal{K} &= C - \frac{1}{\beta^*} \ln(\xi_{\alpha^*} \cdot \xi_{\beta^*}^\perp) + \frac{1}{\beta^*} \int_0^{+\infty} (\beta^* - E_\ell(t)) dt, \\ \mathcal{K}^* &= C^* - \frac{1}{\beta} \ln(\xi_\alpha \cdot \xi_\beta^\perp) + \frac{1}{\beta} \int_0^{+\infty} (\beta - E_{\ell^*}(t)) dt \end{aligned} \quad (2.11)$$

where C and C^* are as in (2.8). We note that the directions of the eigenvectors are such that $\xi_{\alpha^*} \cdot \xi_{\beta^*}^\perp$, $\xi_\alpha \cdot \xi_\beta^\perp > 0$. Both \mathcal{K} and \mathcal{K}^* are well-defined. We also denote

$$J = \{\theta \in I_+ : |\mathcal{D}'(\theta)| \leq 1\}, \quad J^* = \{\theta \in I_+^* : |(\mathcal{D}^*)'(\theta)| \leq 1\}. \quad (2.12)$$

We have

Theorem 2.4 (Transient heteroclinic tangle). *Let $h \in \mathbb{R}^+$ be a real parameter and*

$$\mathcal{D}_h(\theta) := \frac{h}{\beta^*} + \mathcal{K} + \mathcal{D}(\theta), \quad \mathcal{D}_h^*(\theta) := \frac{h}{\beta} + \mathcal{K}^* + \mathcal{D}^*(\theta).$$

If there exists an \tilde{h} sufficiently large, such that

$$\mathcal{D}_{\tilde{h}}(J) \subset I_-^*; \quad \mathcal{D}_{\tilde{h}}^*(J^*) \subset I_-;$$

then there exists an open interval $I_{\tilde{\mu}}$ of μ around $\tilde{\mu} = e^{-\tilde{h}}$, such that for all $\mu \in I_{\tilde{\mu}}$, the corresponding heteroclinic tangle Λ_μ conjugates to a horseshoe of infinitely many branches.

Theorem 2.4 is a theorem of very different nature with respect to Theorem 2.1. For the μ values of Theorem 2.4, the heteroclinic tangle Λ contains *nothing else* but a uniformly hyperbolic horseshoe. Since the attractive basin of a uniformly hyperbolic horseshoe is a Lebesgue measure zero set, the heteroclinic tangles of Theorem 2.4 contain no Gibbs measure. These heteroclinic tangles appear transient, that is, they are not directly observable in numerical simulations.

The conditions of Theorems 2.1–2.4 are all *explicit* and *verifiable* for a given set of equations. Through these theorems we have successfully applied various profound dynamics theories on maps, such as the Newhouse theory, the theory of SRB measures and the theory of Hénon-like attractors, to the analysis of a given set of time-periodic differential equations with a heteroclinic tangle.

We finish this section by noting that, instead of pushing for the strongest results possible, in this section we have sometimes traded stronger than necessary assumptions for technical simplicity. In particular, we note that (H2)(ii) is introduced mainly to ease what would otherwise be longer derivations of the separatrix map. Theorems 2.1–2.4 remain valid without assuming (H2)(ii). The smoothness of the forcing functions $P(x, y, t)$, $Q(x, y, t)$, and the infinite order of the non-resonance relations assumed in (H1) for α and β , α^* and β^* , are also stronger than necessary. They can both be reduced to certain finite order. We also note that (H3)(ii) is obviously an overkill for Theorem 2.1. For Theorem 2.1 to hold it suffices to assume that there exist one non-tangential zero for $\mathcal{W}(\theta)$ and one for $\mathcal{W}^*(\theta)$. Finally, we obtain the corresponding theorems for homoclinic tangles by letting $\mathcal{W}(\theta) = \mathcal{W}^*(\theta)$.

3. The separatrix map

The main tool of our study is the separatrix map induced by the solutions of (2.3) around the unforced heteroclinic loop $\ell \cup \ell^*$, which we rigorously derive from Eq. (2.3). The detailed derivations of the separatrix map are a little tedious, and thus are presented in Appendix A. In this section we present only the end results. A list of quantities is involved in this presentation; some are less than straightforward to motivate. The presented formula for the separatrix map might appear a little messy at first sight. Digestive remarks are included to explain the implications of the various quantities involved.

Let $B_\varepsilon(P)$ be the ε -ball centered at P and $B_{\varepsilon^*}(P^*)$ be the ε^* -ball centered at P^* in the (x, y) -plane. Let L_- be such that $|\ell(-L_-) - P| = \frac{1}{2}\varepsilon$ and L_+ be such that $|\ell(L_+) - P^*| = \frac{1}{2}\varepsilon^*$. Similarly, L_-^* is by $|\ell^*(-L_-^*) - P^*| = \frac{1}{2}\varepsilon^*$, L_+^* by $|\ell^*(L_+^*) - P| = \frac{1}{2}\varepsilon$.

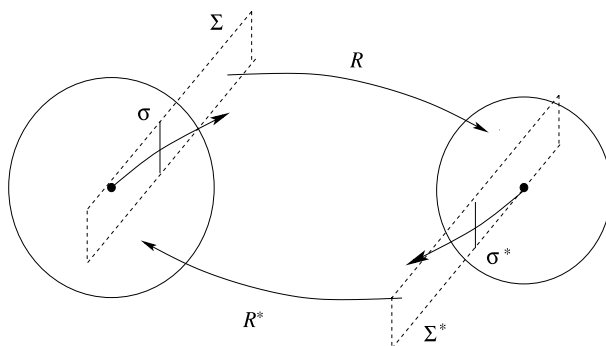


Fig. 3. $\mathcal{R}, \mathcal{R}^*$ in the extended phase space.

Let σ, σ^* be two short segments of size $\approx 2\mu$ centered at $\ell(-L_-)$ and $\ell^*(-L_-^*)$ respectively in the (x, y) -plane. All tangent vectors of σ are roughly aligned to ξ_α and those of σ^* to ξ_{α^*} . In what follows, Σ is a surface that is C^r -close to $\sigma \times S^1$ and Σ^* is a surface that is C^r -close to $\sigma^* \times S^1$ in the extended phase space where $r > 3$ is an arbitrarily fixed integer. For all practical purposes, let us at the moment think of Σ as $\sigma \times S^1$ and Σ^* as $\sigma^* \times S^1$. We denote the map induced by the solutions of Eq. (2.3) from Σ to Σ^* as $\mathcal{R} = \mathcal{R}_\mu$, and the map from Σ^* back to Σ as $\mathcal{R}^* = \mathcal{R}_\mu^*$. The separatrix map $\mathcal{F} = \mathcal{F}_\mu : \Sigma \rightarrow \Sigma$ is such that $\mathcal{F}_\mu = \mathcal{R}_\mu^* \circ \mathcal{R}_\mu$.

In this section we introduce pseudo-explicit formulas for \mathcal{R} and \mathcal{R}^* . We then prove Theorems 2.1–2.4 by using the asserted formulas in the next section. Detailed derivations of the formulas asserted are presented in Appendix A. We start with some notation and definition of parameters.

Parameters $\varepsilon, \varepsilon^*$ and μ . Let $\varepsilon, \varepsilon^*$ be such that

$$\varepsilon^* = \varepsilon^{\frac{\beta^*}{\beta}}; \quad (3.1)$$

and $\varepsilon, \varepsilon^*$ are sufficiently small such that, on $B_\varepsilon(P)$ and $B_{\varepsilon^*}(P^*)$, Eq. (2.3) can be linearized. The quantities L_\pm, L_\pm^* are completely determined by ℓ, ℓ^* and $\varepsilon, \varepsilon^*$.

The parameter μ controls the magnitude of the time-periodic perturbation and we assume

$$\mu \ll \varepsilon, \quad \varepsilon^* \ll 1. \quad (3.2)$$

The new parameter $h = \ln \mu^{-1}$. We need to estimate the derivatives with respect to a forcing parameter but in this case μ is not a good choice, for taking derivatives with respect to μ would create non-perturbational terms from the forcing function in the variational equations. To deal with this problem we would let $h = \ln \mu^{-1}$ and regard h , not μ , as the bottom-line parameter. In other words, we would regard μ as a shorthand for e^{-h} , and take all functions in μ as functions in h . Observe that $(0, \mu_0)$ for μ corresponds to the interval $(\ln \mu_0^{-1}, +\infty)$ for h . By regarding a function $F(\mu)$ of μ as a function of h ,

$$\partial_h F(\mu) = -\mu \partial_\mu F(\mu),$$

and this would allow us to keep a much needed copy of μ in front.

The use of generic constant K . The letter K is used throughout to generically represent constants that are independent of μ . The precise value of K is allowed to change from line to line. On occasions, a specific constant is used in different places. There are also times we need to distinguish two K 's in the same line. We would then use subscripts to denote them as K_0, K_1, \dots . We would also make

distinctions between constants that are dependent on ε , ε^* and those that are not by making such dependency explicit. A constant that depends on ε and ε^* is written as $K(\varepsilon)$ or $K(\varepsilon^*)$. A constant written as K is independent of ε and ε^* .

The use of \mathcal{O} -terms. The intended formula for the separatrix map would inevitably contain terms that are explicit and terms that are implicit. Implicit terms are usually “error” terms, and the usefulness of a derived formula would depend completely on how well the error terms are controlled. We aim at C^r -control on all error terms with respect to all variables in the extended phase space for some $r > 3$. To facilitate our presentation, we adopt specific conventions to indicate controls on magnitude. For a given constant, we write $\mathcal{O}(1)$, $\mathcal{O}(\varepsilon)$ or $\mathcal{O}(\mu)$ to indicate that the magnitude of the constant is bounded by K , $K\varepsilon$ or $K(\varepsilon)\mu$, respectively. For a function of a set V of variables, we write $\mathcal{O}_V(1)$, $\mathcal{O}_V(\varepsilon)$ or $\mathcal{O}_V(\mu)$ to represent a function, the C^r -norm of which in V are bounded by K , $K\varepsilon$ or $K(\varepsilon)\mu$, respectively. For example, $\mathcal{O}_{Z,\theta}(\mu)$ represents a function of Z , θ , the C^r -norm of which with respect to Z and θ are bounded above by $K(\varepsilon)\mu$.

Variables for Σ and Σ^* . To present the formulas for $\mathcal{R} : \Sigma \rightarrow \Sigma^*$ and $\mathcal{R}^* : \Sigma^* \rightarrow \Sigma$, we need to first introduce coordinates on Σ and Σ^* . We observe that Σ is an annulus, the points of which we first represent by using two variables X and θ where X is, roughly speaking, the distance from a point on Σ to $\ell(-L_-) \times S^1$ and $\theta \in S^1$. We then re-scale X by letting $\mathbb{X} = \mu^{-1}X$. This way we represent Σ by letting

$$\Sigma = \{(\mathbb{X}, \theta) : |\mathbb{X}| < 1, \theta \in S^1\}.$$

Coordinates for Σ^* are defined in a similar fashion as

$$\Sigma^* = \{(\hat{\mathbb{X}}, \hat{\theta}) : |\hat{\mathbb{X}}| < 1, \hat{\theta} \in S^1\}.$$

On M_{\pm} , M_{\pm}^* , $\mathcal{W}_{L_-, L_+}(\theta)$ and $\mathcal{W}_{L_+^*, L_+^*}^*(\theta)$. In addition to L_{\pm} , L_{\pm}^* , α , α^* , β , β^* , ε , ε^* and $h = \ln \mu^{-1}$, we also need four more constants M_{\pm} , M_{\pm}^* , where they are defined as

$$M_+ = e^{\int_0^{L_+} E_{\ell}(s) ds}, \quad M_- = e^{\int_{-L_-}^0 E_{\ell}(s) ds};$$

and

$$M_+^* = e^{\int_0^{L_+^*} E_{\ell^*}(s) ds}, \quad M_-^* = e^{\int_{-L_-^*}^0 E_{\ell^*}(s) ds}.$$

Finally, we define $\mathcal{W}_{L_-, L_+}(\theta)$ by replacing the integral bounds $+\infty$, $-\infty$ in (2.4) for $\mathcal{W}(\theta)$ by using L_+ , $-L_-$ respectively. The function $\mathcal{W}_{L_+^*, L_+^*}^*(\theta)$ is similarly defined.

For $\mathcal{R} : \Sigma \rightarrow \Sigma^*$ we have

Proposition 3.1 (Formula for \mathcal{R}). Let the map $\mathcal{R} : \Sigma \rightarrow \Sigma^*$ be denoted as

$$(\hat{\mathbb{X}}, \hat{\theta}) = \mathcal{R}(\mathbb{X}, \theta).$$

We have

$$\begin{aligned} \hat{\theta} &= \theta + \mathbf{a} - \frac{1}{\beta^*} \ln \mathbb{F}(\theta, \mathbb{X}, \mu) + \mathcal{O}_{\theta, \mathbb{X}, h}(\mu), \\ \hat{\mathbb{X}} &= \mathbf{b} [\mathbb{F}(\theta, \mathbb{X}, \mu)]^{-\frac{\alpha^*}{\beta^*}} \end{aligned} \quad (3.3)$$

where

$$\mathbb{F}(\theta, \mathbb{X}, \mu) = \mathcal{W}(\theta + L_-) - M_- (1 + \mathcal{O}(\varepsilon^*)) (\xi_\alpha \cdot \xi_\beta^\perp) \mathbb{X} + \mathbb{E}(\theta) + \mathcal{O}_{\theta, \mathbb{X}, h}(\mu) \quad (3.4)$$

in which

$$\mathbb{E}(\theta) = ((M_+)^{-1} + M_-) \mathcal{O}_\theta(1) + \mathcal{W}_{L_-, L_+}(\theta + L_-) - \mathcal{W}(\theta + L_-). \quad (3.5)$$

We also have

$$\begin{aligned} \mathbf{a} &= \frac{1}{\beta^*} \left(\ln \mu^{-1} + \ln \frac{\varepsilon^*}{(1 + \mathcal{O}(\varepsilon^*)) M_+} - \ln(\xi_{\alpha^*} \cdot \xi_{\beta^*}^\perp) \right) + (L_- + L_+); \\ \mathbf{b} &= (\mu(\varepsilon^*)^{-1})^{-\frac{\alpha^*}{\beta^*} - 1} [(1 + \mathcal{O}(\varepsilon^*)) M_+]^{-\frac{\alpha^*}{\beta^*}}. \end{aligned} \quad (3.6)$$

Similarly, for $\mathcal{R}^* : \Sigma^* \rightarrow \Sigma$ we have

Proposition 3.2 (Formula for \mathcal{R}^*). Let the map $\mathcal{R}^* : \Sigma^* \rightarrow \Sigma$ be denoted as

$$(\mathbb{X}, \theta) = \mathcal{R}^*(\hat{\mathbb{X}}, \hat{\theta}).$$

We have

$$\begin{aligned} \theta &= \hat{\theta} + \mathbf{a}^* - \frac{1}{\beta} \ln \mathbb{F}^*(\hat{\theta}, \hat{\mathbb{X}}, \mu) + \mathcal{O}_{\hat{\theta}, \hat{\mathbb{X}}, h}(\mu), \\ \mathbb{X} &= \mathbf{b}^* [\mathbb{F}^*(\hat{\theta}, \hat{\mathbb{X}}, \mu)]^{-\frac{\alpha}{\beta}} \end{aligned} \quad (3.7)$$

where

$$\mathbb{F}^*(\hat{\theta}, \hat{\mathbb{X}}, \mu) = \mathcal{W}^*(\hat{\theta} + L_-^*) - M_-^* (1 + \mathcal{O}(\varepsilon)) (\xi_{\alpha^*} \cdot \xi_{\beta^*}^\perp) \hat{\mathbb{X}} + \mathbb{E}^*(\hat{\theta}) + \mathcal{O}_{\hat{\theta}, \hat{\mathbb{X}}, h}(\mu) \quad (3.8)$$

in which

$$\mathbb{E}^*(\hat{\theta}) = ((M_+^*)^{-1} + M_-^*) \mathcal{O}_{\hat{\theta}}(1) + \mathcal{W}_{L_-^*, L_+^*}^*(\hat{\theta} + L_-^*) - \mathcal{W}^*(\hat{\theta} + L_-^*). \quad (3.9)$$

We also have

$$\begin{aligned} \mathbf{a}^* &= \frac{1}{\beta} \left(\ln \mu^{-1} + \ln \frac{\varepsilon}{(1 + \mathcal{O}(\varepsilon)) M_+^*} - \ln(\xi_\alpha \cdot \xi_\beta^\perp) \right) + (L_-^* + L_+^*); \\ \mathbf{b}^* &= (\mu \varepsilon^{-1})^{-\frac{\alpha}{\beta} - 1} [(1 + \mathcal{O}(\varepsilon)) M_+^*]^{-\frac{\alpha}{\beta}}. \end{aligned} \quad (3.10)$$

Digestive remarks. We offer the following remarks on (3.3) for \mathcal{R} and (3.7) for \mathcal{R}^* in the two propositions above.

- (i) Observe that $\mathbf{b}, \mathbf{b}^* \rightarrow 0$ as $\mu \rightarrow 0$, for we have assumed that $|\alpha| > \beta$, $|\alpha^*| > \beta^*$. Hence for $\mu > 0$ sufficiently small, we can think of $\mathcal{R} : \Sigma \rightarrow \Sigma^*$ as a 2D family of maps unfolded from the following 1D maps $f = f_\mu : S^1 \rightarrow S^1$ where

$$f_\mu(\theta) = \theta + \mathbf{a} - \frac{1}{\beta^*} \ln(\mathcal{W}(\theta + L_-) + \mathbb{E}(\theta)).$$

Similarly, $\mathcal{R}^* : \Sigma^* \rightarrow \Sigma$ is a 2D family of maps unfolded from the 1D map $f^* = f_\mu^* : S^1 \rightarrow S^1$ where

$$f_\mu^*(\theta) = \theta + \mathbf{a}^* - \frac{1}{\beta} \ln(\mathcal{W}^*(\theta + L_-^*) + \mathbb{E}^*(\theta)).$$

We can also regard the separatrix map \mathcal{F} as a 2D family unfolded from the 1D map $F_\mu = f_\mu^* \circ f_\mu$. The functions $f_\mu(\theta)$, $f_\mu^*(\theta)$ and $F_\mu(\theta)$ are the respective 1D singular limit for \mathcal{R} , \mathcal{R}^* and \mathcal{F} .

- (ii) Regard ε and ε^* as fixed constants and let $\mu \rightarrow 0$. Recall that $h = \ln \mu^{-1}$ is the parameter representing μ and we have $\mathbf{a} \approx \beta^{*-1}h$, $\mathbf{a}^* \approx \beta^{-1}h$. The 1D singular limit f_μ , f_μ^* and $F_\mu = f_\mu^* \circ f_\mu$ for the separatrix map take h as a parameter and $h = \ln \mu^{-1} \rightarrow \infty$ as $\mu \rightarrow 0$. Sometimes we also denote the 1D singular limit as f_h , f_h^* and F_h respectively.
- (iii) We have

$$L_- + C \approx L_-^* + C^*$$

from (3.1) and (2.8). We also have, for M_\pm, M_\pm^* ,

$$M_+ \sim (\varepsilon^*)^{\frac{\beta^*}{\alpha^*}}, \quad M_- \sim \varepsilon^{-\frac{\alpha}{\beta}}; \quad M_+^* \sim \varepsilon^{\frac{\beta}{\alpha}}, \quad M_-^* \sim (\varepsilon^*)^{-\frac{\alpha^*}{\beta^*}}.$$

It is then clear that $M_-, M_-^* \gg \mathcal{O}(\mu)$ and a direct consequence is that

$$\frac{\partial}{\partial \mathbb{X}} \mathbb{F}(\theta, \mathbb{X}, \mu) \approx M_- (\xi_\alpha \cdot \xi_\beta^\perp); \quad \frac{\partial}{\partial \hat{\mathbb{X}}} \mathbb{F}^*(\theta, \hat{\mathbb{X}}, \mu) \approx M_-^* (\xi_{\alpha^*} \cdot \xi_{\beta^*}^\perp).$$

This is to say that the unfolding from the 1D singular limit $F = f^* \circ f$ to the separatrix map $\mathcal{F} = \mathcal{R}^* \circ \mathcal{R}$ is non-degenerate in the \mathbb{X} -direction.

- (iv) Using (iii) and (3.1) for ε and ε^* , we also have

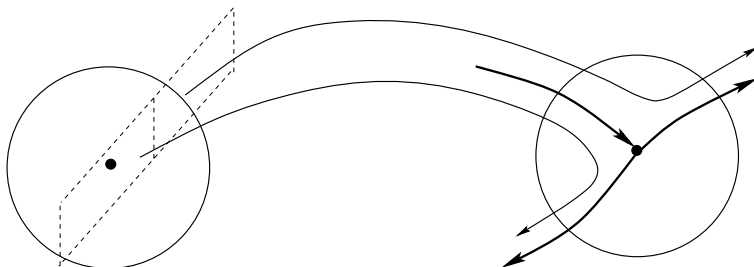
$$\mathbf{a} \approx \frac{1}{\beta^*} \ln \mu^{-1} + \mathcal{K}, \quad \mathbf{a}^* \approx \frac{1}{\beta} \ln \mu^{-1} + \mathcal{K}^*$$

where \mathcal{K} and \mathcal{K}^* are as in (2.11).

- (v) It is also easy to prove that

$$\|\mathcal{W}(\theta) - \mathcal{W}_{L_-, L_+}(\theta)\|_{C^r}, \quad \|\mathcal{W}^*(\theta) - \mathcal{W}_{L_-^*, L_+^*}^*(\theta)\|_{C^r} \rightarrow 0$$

as $\varepsilon, \varepsilon^* \rightarrow 0$. Together with (iii) we conclude that, when $\varepsilon, \varepsilon^*$ are sufficiently small, $\mathbb{E}(\theta)$, $\mathbb{E}^*(\hat{\theta})$ are C^r -small perturbations to $\mathcal{W}(\theta)$, $\mathcal{W}^*(\hat{\theta})$, respectively.

Fig. 4. Partial definition of \mathcal{R} on Σ .

4. Dynamics of heteroclinic tangles

Recall that $\mathcal{F} = \mathcal{R}^* \circ \mathcal{R} : \Sigma \rightarrow \Sigma$ is the separatrix map and the heteroclinic tangle $\Lambda = \Lambda_\mu$ is such that

$$\Lambda_\mu = \{(\mathbb{X}, \theta) \in \Sigma : \mathcal{F}^n(\mathbb{X}, \theta) \in \Sigma \text{ for all } n \in \mathbb{Z}\}.$$

In this section, we study the geometrical and the dynamical structure of Λ_μ through Propositions 3.1 and 3.2.

4.1. Geometry of the separatrix map

Let $\Sigma = I \times S^1$. Points in $I = [-1, 1]$ are denoted by using \mathbb{X} and points in $S^1 = \mathbb{R}/\{nT\}$ are denoted by using θ . We call the direction of θ the *horizontal direction* and the direction of \mathbb{X} the *vertical direction*.

We start with the simple fact that \mathcal{R} is only partially defined on Σ , for after reaching $B_{\varepsilon^*}(P^*)$, a solution could follow either ℓ^* to reach Σ^* or the other unstable branch of P^* to leave the neighborhood of $\ell \cup \ell^*$. See Fig. 4. Reflected in Proposition 3.1 for \mathcal{R} is the logarithmic function in (3.3), and \mathcal{R} is defined only on the part of Σ where the value of the function inside of the logarithm is positive.

Let U be the subset of Σ where \mathcal{R} is defined. We use Proposition 3.1 to determine the geometry of U in Σ . Note that U is defined by $\mathbb{F}(\theta, \mathbb{X}, \mu) > 0$ where $\mathbb{F}(\theta, \mathbb{X}, \mu)$ is as in (3.4). The boundaries of U in Σ are defined by the equation

$$\mathbb{F}(\theta, \mathbb{X}, \mu) = \mathcal{W}(\theta + L_-) - M_-(1 + \mathcal{O}(\varepsilon^*))(\xi_\alpha \cdot \xi_\beta^\perp)\mathbb{X} + \mathbb{E}(\theta) + \mathcal{O}_{\theta, \mathbb{X}, h}(\mu) = 0,$$

from which it follows that

$$\mathbb{X} = \frac{1}{M_-(1 + \mathcal{O}(\varepsilon^*))(\xi_\alpha \cdot \xi_\beta^\perp)}(\mathcal{W}(\theta + L_-) + \mathbb{E}(\theta)) + \mathcal{O}_{\theta, h}(\mu). \quad (4.1)$$

We claim that (4.1) defines a finite collection of vertical curves located roughly at the zeros of the Melnikov function $\mathcal{W}(\theta + L_-)$. This is because (a) $M_- \approx \varepsilon^{-\frac{\alpha}{\beta}}$ (digestive remark (iii) at the end of Section 3); (b) the intersections of the graph of $\mathcal{W}(\theta)$ with the θ -axis are non-tangential (this is (H3)(ii)); and (c) $\mathbb{E}(\theta)$ is a C^r -small perturbation to $\mathcal{W}(\theta + L_-)$ (digestive remark (v) at the end of Section 3). It then follows that U is a finite collection of vertical strips. Let $U = \bigcup U_i$ where U_i are the vertical strips in Σ , and $W = \Sigma \setminus U$. The sets U and W contain equal number of alternating vertical strips in Σ .

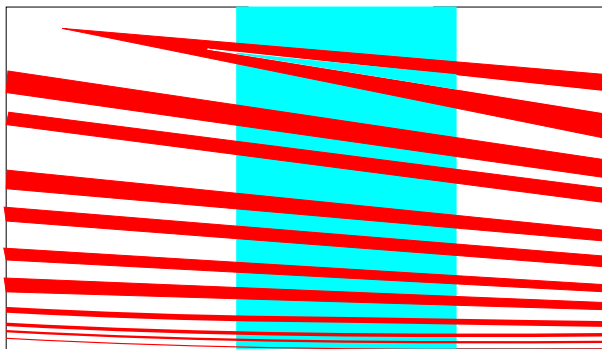


Fig. 5. The geometry of $\mathcal{R}(U_i)$.

Next we study the geometry of $\mathcal{R}(U_i)$ in Σ^* . First let l_i be the intersection of U_i with the θ -axis. Then $\mathcal{R}(l_i)$ by (3.3) is a curve in Σ^* , extending in the horizontal direction to $\theta = +\infty$ toward both end. The shape of $\mathcal{R}(l_i)$ copies the shape of the dynamical function

$$\mathcal{D}(\theta) = \theta - \frac{1}{\beta^*} \ln \mathcal{W}(\theta + L_-)$$

on the corresponding θ -interval. It also follows from (3.3) that $\mathcal{R}(U_i)$ is a slight thickening of $\mathcal{R}(l_i)$ in Σ^* . Viewing Σ^* as an annulus, we see that the image of $\mathcal{R}(U_i)$ wraps around Σ^* infinitely many times. See Fig. 5.

Proposition 3.1 also tells how $\mathcal{R}(U_i)$ moves in Σ^* as $\mu \rightarrow 0$. Observe that $(\beta^*)^{-1} \ln \mu^{-1}$ appears as a simple additive term in **a** for the angular variable $\hat{\theta}$ in (3.3). This implies that, as $\mu \rightarrow 0$, $\mathcal{R}(U_i)$ moves horizontally in Σ^* with a roughly constant speed $(\beta^*)^{-1}$ with respect to $h = \ln \mu^{-1}$. We also note that $\mathcal{R}(U_i)$ for all i are tied together and they move with the same horizontal speed in Σ^* .

In summary, Proposition 3.1 for \mathcal{R} has revealed that: (1) \mathcal{R} is defined on a finite collection of vertical strips; (2) the image of each of these vertical strips in Σ^* has the shape of the dynamical function $\mathcal{D}(\theta)$ and it wraps around the annulus Σ^* infinitely many times; and (3) as $\mu \rightarrow 0$, these infinitely wrapped images move in the θ -direction in Σ^* with a roughly constant speed of $(\beta^*)^{-1}$ with respect to $h = \ln \mu^{-1}$.

The situation for \mathcal{R}^* is completely parallel. This is to say that (1) \mathcal{R}^* is defined on a finite collection of vertical strips in Σ^* , which we denote as $U^* = \bigcup U_i^*$; (2) the image of each of these vertical strips in Σ is in the shape of the dynamical function $\mathcal{D}^*(\theta)$ and it wraps around the annulus Σ infinitely many times; and (3) as $\mu \rightarrow 0$, these infinitely wrapped images move in the θ -direction in Σ with a roughly constant speed of β^{-1} with respect to $h = \ln \mu^{-1}$.

4.2. Intrinsic phases

Let us be aware that ε and μ are parameters of completely different nature: μ is a parameter that really changes the dynamics of the system while ε is entirely *auxiliary* in the sense that it is a technical artifact of our derivation process. On the other hand, we observe that the formulas for \mathcal{R} and \mathcal{R}^* in Section 3 appear to depend on ε non-trivially through L_\pm and L_\pm^* . If the conclusion of our propositions are to be correct, then this non-trivial dependency on ε must be somewhat illusory, and there should be quantities that are *intrinsic* in the sense that they are independent of ε and they ultimately determine the dynamics of $\mathcal{F} = \mathcal{R}^* \circ \mathcal{R}$. This is indeed the case and the intrinsic quantities are $C, C^*, \mathcal{K}, \mathcal{K}^*$ in Section 2. These are the *intrinsic phases* for \mathcal{R} and \mathcal{R}^* , which we obtain through (3.3) and (3.7).

To see through this illusory dependency of \mathcal{R} and \mathcal{R}^* in (3.3) and (3.7) on ε , we first observe that the parameters \mathbf{a} and \mathbf{a}^* are such that

$$\mathbf{a} \approx \frac{1}{\beta^*} \ln \mu^{-1} + \mathcal{K}, \quad \mathbf{a}^* \approx \frac{1}{\beta} \ln \mu^{-1} + \mathcal{K}^*.$$

See the digestive remark (iv) at the end of Section 3.

Second we change θ to $\theta - (L_- + C)$ on both Σ and Σ^* . Observe that (1) this does not change any of the constants in (3.3) and (3.7); (2) $\mathcal{O}_{\theta, \mathbb{X}, h}(\mu)$ and $\mathcal{O}_\theta(1)$ in (3.3) and (3.7) can be written as the same; and (3) a simple shift on θ does not alter the fact that $\mathbb{E}(\theta)$, $\mathbb{E}^*(\theta)$ are C^r -small perturbations of the corresponding Melnikov functions. For notational simplicity let us write $\mathbb{E}(\theta - L_- - C)$ and $\mathbb{E}^*(\theta - L_- - C)$ back as $\mathbb{E}(\theta)$ and $\mathbb{E}^*(\theta)$ respectively.

Therefore the new formulas for \mathcal{R} and \mathcal{R}^* are as follows: Everything else are kept the same as in Propositions 3.1 and 3.2, but we now change $\mathcal{W}(\theta + L_-)$ to $\mathcal{W}(\theta - C)$, and $\mathcal{W}^*(\theta + L_-^*)$ to $\mathcal{W}^*(\theta - C^* + (L_-^* + C^* - L_- - C))$, which is $\approx \mathcal{W}^*(\theta - C^*)$ because $L_- + C \approx L_-^* + C^*$ (see the digestive remark (iii) at the end of Section 3). This is to say that we are allowed to change $\mathbb{F}(\theta, \mathbb{X}, \mu)$ in (3.4) to

$$\mathbb{F}(\theta, \mathbb{X}, \mu) = \mathcal{W}(\theta - C) - M_-(1 + \mathcal{O}(\varepsilon^*))(\xi_\alpha \cdot \xi_\beta^\perp) \mathbb{X} + \mathbb{E}(\theta) + \mathcal{O}_{\theta, \mathbb{X}, h}(\mu) \quad (4.2)$$

and $\mathbb{F}^*(\theta, \mathbb{X}, \mu)$ in (3.8) to

$$\mathbb{F}^*(\hat{\theta}, \hat{\mathbb{X}}, \mu) = \mathcal{W}^*(\hat{\theta} - C^* + c) - M_-^*(1 + \mathcal{O}(\varepsilon))(\xi_{\alpha^*} \cdot \xi_{\beta^*}^\perp) \hat{\mathbb{X}} + \mathbb{E}^*(\hat{\theta}) + \mathcal{O}_{\hat{\theta}, \hat{\mathbb{X}}, h}(\mu) \quad (4.3)$$

where

$$c = L_-^* + C^* - L_- - C \approx 0.$$

4.3. Dynamical consequences

We start with what we will call as the *quasi-periodicity* of dynamical behavior of the heteroclinic tangles implicated by (3.3) and (3.7). Recall that $h = \ln \mu^{-1}$ and let

$$\begin{aligned} f_h(\theta) &= \theta + \frac{1}{\beta^*} h + \mathcal{K} - \frac{1}{\beta^*} \ln \mathcal{W}(\theta - C), \\ f_h^*(\theta) &= \theta + \frac{1}{\beta} h + \mathcal{K}^* - \frac{1}{\beta} \ln \mathcal{W}^*(\theta - C^*). \end{aligned} \quad (4.4)$$

The 1D function $f_h(\theta)$ is the 1D singular limit for \mathcal{R} , and $f_h^*(\theta)$ is for \mathcal{R}^* . Note that $f_h(\theta)$ and $f_h^*(\theta)$ are not exactly the same 1D maps as $f(\theta)$ and $f^*(\theta)$ that appeared previously in the digestive remark (i) at the end of Section 3. We have replaced \mathbf{a} by $\frac{1}{\beta^*} h + \mathcal{K}$, \mathbf{a}^* by $\frac{1}{\beta} h + \mathcal{K}^*$, $\mathcal{W}(\theta + L_-)$ by $\mathcal{W}(\theta - C)$ and $\mathcal{W}^*(\theta + L_-^*)$ by $\mathcal{W}^*(\theta - C^*)$. The reasons for these replacements have been explained in detail in the previous subsection. We have also dropped the error functions $\mathbb{E}(\theta)$ and $\mathbb{E}^*(\theta)$; see digestive remark (v) at the end of Section 3. We call the circular map $F_h = f_h^* \circ f_h : S^1 \rightarrow S^1$ the *intrinsic* 1D singular limit for the separatrix map $\mathcal{F} = \mathcal{R}^* \circ \mathcal{R}$.

Regarding h as a parameter, $f_h : S^1 \rightarrow S^1$ is such that $f_h = f_{h+\beta^* T}$ where T is the period of the forcing function. This is to say that, as a one parameter family, $f_h : S^1 \rightarrow S^1$ is periodic of period $\beta^* T$ in h . Through $h = \ln \mu^{-1}$, this *additive* periodicity in h is transformed to a *multiplicative* periodicity in μ . This is to say that for any given μ_0 sufficiently small, f_h is the same for μ_0 and $\mu_1 = \mu_0 e^{-\beta^* T}$. We call $e^{\beta^* T}$ the *multiplicative period* for f_h in μ . Similarly, $f_h^*(\theta)$ is a one parameter family of circle maps with a multiplicative period $e^{\beta T}$ in μ . For $F_h = f_h^* \circ f_h$, we have

Case 1. If β and β^* are rationally related, this is to say that, if there are $m, n \in \mathbb{Z}^+$, relatively prime, such that

$$\frac{\beta}{\beta^*} = \frac{m}{n}.$$

Then F_h is such that

$$F_h = F_{h+n\beta T} = F_{h+m\beta^* T}$$

and the multiplicative period for F_h in μ is $e^{n\beta T}$ (also $= e^{m\beta^* T}$).

Case 2. If β and β^* are not rationally related, then F_h is not periodic in h .

Therefore, if the unstable eigenvalues β and β^* are rationally related, then the dynamical behavior of the heteroclinic tangles are with a repetitive pattern for small μ that is intrinsic in the sense that it becomes more and more precise as $\mu \rightarrow 0$. The length of the period in $h = \ln \mu^{-1}$ depends on β, β^* and their order of resonance. If β and β^* are non-resonant, then the repetitive pattern of dynamical behavior ceases to exist.

We now move on to the proofs of Theorems 2.1–2.4.

Proof of Theorem 2.1. Instead of (H3), for Theorem 2.1 we only need one non-tangential zero for $\mathcal{W}(\theta)$ and one more for $\mathcal{W}^*(\theta)$, which we denote as θ_0 and θ_0^* respectively. Let $\mathbb{F} = \mathbb{F}(\theta, \mathbb{X}, \mu)$ be as in (4.2). It then follows that $\mathbb{F} = 0$ defines a vertical curve in Σ close to $\theta = \theta_0 + C$, which we denote as ℓ_v . ℓ_v is isolated in the sense that $\mathbb{F} = 0$ has no other solution in a sufficiently small neighborhood of ℓ_v . In addition, the sign of \mathbb{F} changes from one side of ℓ_v to the other in Σ . We shift ℓ_v slightly in the horizontal direction to the side where $\mathbb{F}(\theta, \mathbb{X}, \mu)$ is positive and denote the resulting vertical curve as $\tilde{\ell}_v$. The vertical strip bounded by ℓ_v and $\tilde{\ell}_v$, we denote as \tilde{U} . For $z = (\theta, \mathbb{X}) \in \tilde{U}$, we denote the horizontal cone formed by all tangent vectors of slope $< \frac{1}{100}$ as $C_h(z)$ and the vertical cone formed by all tangent vectors of slope > 100 as $C_v(z)$, where the slope is defined as the absolute value of the ratio of the \mathbb{X} -component over the θ -component. Similarly, we obtain $\ell_v^*, \tilde{\ell}_v^*, \tilde{U}^*$ close to $\theta = \theta_0^* + C^*$ in Σ^* .

The horizontal boundaries of \tilde{U} are defined by $\mathbb{X} = -1$ and $\mathbb{X} = 1$, and the vertical boundaries are defined by ℓ_v and $\tilde{\ell}_v$. We call a smooth, non-self-intersecting curve in \tilde{U} a vertical curve if all its tangent vectors are in C_v and it connects the two horizontal boundaries of \tilde{U} . Two non-intersecting vertical curves bound a vertical strip. Let $V \subset \tilde{U}$ be a vertical strip. We call a smooth, non-self-intersecting curve in \tilde{U} a horizontal curve if all its tangent vectors are in C_h and it connects the two vertical boundaries of V . Two non-intersecting horizontal curves in V form a horizontal strip in V . The same terms are similarly defined on \tilde{U}^* . We also let $D\mathcal{R}$ be the Jacobian matrix of $\mathcal{R} : \tilde{U} \rightarrow \Sigma^*$, and $D\mathcal{R}^*$ be the Jacobian matrix of $\mathcal{R}^* : \tilde{U}^* \rightarrow \Sigma$. It is straightforward to verify by using (3.3) and (3.7) for \mathcal{R} and \mathcal{R}^* that

- (a) (*Horizontal and vertical strips*) $\mathcal{R}(\tilde{U}) \cap \tilde{U}^* = \bigcup_{i=1}^{+\infty} H_i^*$, where $\{H_i^*\}$ is a sequence of horizontal strips in \tilde{U}^* , monotonically accumulating to $\{\mathbb{X} = 0\}$ as $i \rightarrow +\infty$. Let $V_i = \mathcal{R}^{-1}(H_i^*)$. Then $\{V_i\}$ is a sequence of vertical strips in \tilde{U} , monotonically accumulating to ℓ_v as $i \rightarrow +\infty$. For \mathcal{R}^* , $\{H_i\}$ are such that $\mathcal{R}^*(\tilde{U}^*) \cap \tilde{U} = \bigcup_{i=1}^{+\infty} H_i$ and $\{V_i^*\}$ are such that $V_i^* = (\mathcal{R}^*)^{-1}(H_i)$.
- (b) (*Unstable invariant cone condition*) There exists a constant $\lambda > 1$, such that

$$D\mathcal{R}_z(C_h(z)) \subset C_h(\mathcal{R}(z))$$

for all $z \in \tilde{U}$ and

$$|D\mathcal{R}_z(\tau)| > \lambda|\tau|$$

for all $\tau \in C_h(z)$. Similarly, we have $D\mathcal{R}_z^*(C_h(z)) \subset C_h(\mathcal{R}^*(z))$ for all $z \in \tilde{U}^*$ and $|D\mathcal{R}_z^*(\tau)| > \lambda|\tau|$ for all $\tau \in C_h(z)$.

- (c) (*Stable invariant cone condition*) There exists a constant $\lambda > 1$, such that if $z \in \tilde{U}$ is such that $\mathcal{R}(z) \in \tilde{U}^*$, then

$$D\mathcal{R}_{\mathcal{R}(z)}^{-1}(C_v(\mathcal{R}(z))) \subset C_v(z).$$

In addition, for $\tau \in C_v(\mathcal{R}(z))$,

$$|D\mathcal{R}_{\mathcal{R}(z)}^{-1}(\tau)| > \lambda|\tau|.$$

Similarly, if $z \in \tilde{U}^*$ is such that $\mathcal{R}^*(z) \in \tilde{U}$, then $D(\mathcal{R}^*)_{\mathcal{R}^*(z)}^{-1}(C_v(\mathcal{R}^*(z))) \subset C_v(z)$, and in addition we have for $\tau \in C_v(\mathcal{R}^*(z))$, $|D(\mathcal{R}^*)_{\mathcal{R}^*(z)}^{-1}(\tau)| > \lambda|\tau|$.

Items (a)–(c) all follow directly from the simple fact that ℓ_v and ℓ_v^* are defined by using $\mathbb{F} = 0$ and $\mathbb{F}^* = 0$ respectively, around which derivatives of arbitrarily large magnitude in the horizontal direction are asserted by the logarithmic sign in (3.3) and (3.7). Theorem 2.1 follows directly from (a)–(c). See, for example, [14]. \square

Proof of Theorem 2.4. For this theorem to hold we need (H1)–(H3). In particular we need (H3)(ii) and this is to say that all zeros of the Melnikov functions $\mathcal{W}(\theta)$ and $\mathcal{W}^*(\theta)$ are non-tangential. Let $U = \bigcup U_i$ be the domain of \mathcal{R} , where each U_i is bounded by two vertical curves from solving $\mathbb{F} = 0$. Similarly, let $U^* = \bigcup U_j^*$ be the domain of \mathcal{R}^* , where each U_j^* is bounded by two vertical curves from solving $\mathbb{F}^* = 0$. For every U_i , $\mathcal{R}(U_i)$ is a slight thickening of a 1D curve that wraps around Σ^* infinitely many times. We also know that, in the horizontal direction, this 1D curve copies the shape of the dynamical function $\mathcal{D}_h(\theta)$. This is to say that it folds near the critical values of $\mathcal{D}_h(\theta)$ in the horizontal direction. The locations of the folding points of these 1D images are critically important for the dynamics of Λ .

By the assumptions imposed on $D_{\tilde{h}}(\theta)$ and $D_{\tilde{h}}^*(\theta)$, it follows that, for \tilde{h} , all folds of the image $\mathcal{R}(U_i)$ are located in $W^* = \Sigma \setminus U^*$ where \mathcal{R}^* is not defined, and all folds of the image $\mathcal{R}^*(U_j^*)$ are located in $W = \Sigma \setminus U$ where \mathcal{R} is not defined. For \tilde{h} we have actually assumed more: We can verify that if we let $\tilde{U} = U_i$ and $\tilde{U}^* = U_j^*$, then the items (a)–(c) listed above for \mathcal{R} on \tilde{U} and \mathcal{R}^* on \tilde{U}^* in the proof of Theorem 2.1 remain valid. In fact the only technical difference between the current situation and the situation in the previous theorem is that, in the previous case, the magnitude of the derivatives in the horizontal direction is arbitrarily large on $\mathcal{R}^{-1}(\mathcal{R}(\tilde{U}) \cap \tilde{U}^*)$ because of the singularity of the logarithm function, but in the current situation the derivative is only > 1 in magnitude in the horizontal direction. The latter, however, is sufficient for items (a)–(c) to hold. It follows then from (a)–(c) that Λ for $\mathcal{F}_{\tilde{h}}$ is a uniformly hyperbolic horseshoe. See, again, [14]. It is also clear that if the assumptions on \tilde{h} hold for one h , then they also hold for an open interval of h . \square

Proof of Theorem 2.2. This proof uses the fact that the separatrix map $\mathcal{F} = \mathcal{R}^* \circ \mathcal{R}$ is a slight unfolding of the 1D singular limit $F_h = f_h^* \circ f_h$ and the unfolding is non-degenerate in the \mathbb{X} direction where f_h^* and f_h are as in (4.4). The proof goes as follows. We start with a critical point $c \in S^1$ of f_h . Let $h \rightarrow +\infty$, we see $f_h(c)$ wraps around S^1 infinitely many times.

Let I^* be a connected component of $I_+^* = \{\theta \in S^1, \mathcal{W}^*(\theta - C^*) > 0\}$. We take a closed sub-interval $J^* \subset I^*$ such that $\mathcal{D}^*(J^*)$ is monotone and $|\mathcal{D}^*(J^*)| > \frac{\beta^*}{\beta}T + 2T$. Let (h_1, h_2) be such that $\{f_h(c), h \in (h_1, h_2)\} = J^*$, and $\gamma : (h_1, h_2) \rightarrow S^1$ be such that

$$\gamma(h) = f_h^*(f_h(c)).$$

We claim that the image of $\gamma : (h_1, h_2) \rightarrow S^1$ wraps around S^1 more than once. This is because (i) $|h_2 - h_1| < \beta^* |J^*| < \beta^* T$, and (ii) $|\gamma(h_2) - \gamma(h_1)| > |\mathcal{D}^*(J^*)| - \frac{1}{\beta} |h_2 - h_1| > 2T$.

Therefore, there exists an $\tilde{h} \in (h_1, h_2)$ such that $\gamma(\tilde{h}) = c$. By definition $c \in S^1$ is a supercritical fixed point of $F_{\tilde{h}}$. We then verify that $\mathcal{F} = \mathcal{R}^* \circ \mathcal{R}$ for \tilde{h} admits an attractive periodic fixed point close to $(\theta, \mathbb{X}) = (c, 0)$ by using (3.3) and (3.7). We note that because J^* is a closed sub-interval of I^* , $|(f_h^*)'|$ is uniformly bounded on J^* by a constant that is independent of h . We need this upper bound to be independent of h because, to find an attractive fixed point for \mathcal{F} from the supercritical fixed point c for $F_{\tilde{h}}$, we have to impose a lower bound on h that is dependent on the upper bound of $|(f_h^*)'|$ on J^* . For this reason we use J^* , not I^* , to define the parameter interval (h_1, h_2) . \square

Proof of Theorem 2.3. Let us assume without loss of generality that $\mathcal{D}(\theta)$ has a critical point $c \in I_+$ that is not degenerate. Let I_d be a small interval around c such that the second derivative of $\mathcal{D}(\theta)$ on I_d is not zero. Denote $V_d = \{(\theta, \mathbb{X}) : \theta \in I_d\}$. Let U_i be the vertical strip of U (where \mathcal{R} is defined) such that $V_d \subset U_i$. For a given h that is sufficiently large, we know that close to the vertical boundaries of U_i , there are infinitely many saddle fixed points for the separatrix map \mathcal{F} from Theorem 2.1. Pick one and denote it as p . By making p sufficiently close to the boundary of U_i , we obtain a parameter interval (h_1, h_2) around h such that (a) $h_2 - h_1 > 2\beta^* T$; and (b) the saddle fixed point p for \mathcal{F} has a smooth continuation on (h_1, h_2) , which we denote as $p(h) : (h_1, h_2) \rightarrow \Sigma$. For $h \in (h_1, h_2)$, the unstable manifold $W^u(p(h))$ of \mathcal{F} contains a horizontal segment that comes out of $p(h)$ and it extends across V_d . Let $\ell_d(h)$ be the intersection of this horizontal segment with V_d . The image of $\ell_d(h)$ under \mathcal{R} is a folded piece of 1D curve in Σ^* . By $h_2 - h_1 > 2\beta^* T$ in (a), we know that the tip of $\mathcal{R}(\ell_d(h))$ wraps around Σ^* in the θ -direction in a full round.

As in the proof of the previous theorem, we let I^* be a connected component of $I_+^* = \{\theta \in S^1, \mathcal{W}^*(\theta - C^*) > 0\}$, and we take a closed sub-interval $J^* \subset I^*$ so that $\mathcal{D}^*(J^*)$ is monotone and $|\mathcal{D}^*(J^*)| > \frac{\beta^*}{\beta} T + 2T$. We can also require that J^* is such that $|(\mathcal{D}^*)'(\theta)| > 1$ on J^* . This last requirement guarantees that $\mathcal{F}(\ell_d) = \mathcal{R}^*(\mathcal{R}(\ell_d))$ remains a folded curve with a quadratic tip. In Σ^* we let $V_d^* = \{(\theta, \mathbb{X}) : \theta \in J^*\}$. Then there is a sub-interval $(h_1^*, h_2^*) \subset (h_1, h_2)$, so that the tips of $\mathcal{R}(\ell_d(h_1^*))$ and $\mathcal{R}(\ell_d(h_2^*))$ touch the two vertical boundaries of V_d^* respectively. It then follows that, there exists an $h_0 \in (h_1^*, h_2^*)$, such that $\mathcal{F}(\ell_d(h_0))$ touches $W^s(p(h_0))$ tangentially. Therefore, we obtain a homoclinic tangency for \mathcal{F} with $h = h_0$. This tangency is a quadratic tangency because of the assumption that c is a non-degenerate critical point of $\mathcal{D}(\theta)$.

In order to apply the Newhouse theory, however, we need to further prove that the homoclinic tangency obtained above is a transversal tangency. This is to say that we need to prove that as h varies, the tip of $\mathcal{F}(\ell_d(h))$ and $W^s(p(h))$ move at different speeds. This is a rather tedious task, for which we need to evoke the theory on most contracted curves and their stabilities with respect to parameters developed in part I of [30]. Computations involved are a little long, but all are essentially presented in detail in Appendix C of [27]. \square

5. A concrete example of application

In this section we apply the theorems proved in previous sections to a given set of differential equations. In Section 5.1 we introduce the equations under study. In Section 5.2 we apply Theorems 2.1–2.4 to the equations introduced. In Section 5.3 we present the results of a systematic numerical study.

5.1. A given set of differential equations

We start with a second order differential equation

$$\frac{dx}{dt} = 2xy - \eta(x + \gamma x^2), \quad \frac{dy}{dt} = 1 - 2x - y^2 \quad (5.1)$$

where η, γ are constants. Eq. (5.1) has two saddles $P = (0, -1)$, $P^* = (0, 1)$. The eigenvalues for P are $\alpha = -\eta - 2$, $\beta = 2$ and the eigenvalues for P^* are $\alpha^* = -2$, $\beta^* = 2 - \eta$. The corresponding eigenvectors for α and β at $P = (0, -1)$ are

$$\xi_\alpha = \left(\frac{4 + \eta}{\sqrt{20 + 8\eta + \eta^2}}, \frac{2}{\sqrt{20 + 8\eta + \eta^2}} \right), \quad \xi_\beta = (0, 1) \quad (5.2)$$

respectively and the eigenvectors for α^* and β^* at P^* are

$$\xi_{\alpha^*} = (0, -1), \quad \xi_{\beta^*} = \left(\frac{4 - \eta}{\sqrt{20 - 8\eta + \eta^2}}, \frac{-2}{\sqrt{20 - 8\eta + \eta^2}} \right) \quad (5.3)$$

respectively. Eq. (5.1) admits a heteroclinic solution from P to P^* , which we denote as $\ell = (a(t), b(t))$. We have, for all η, γ ,

$$a(t) = 0, \quad b(t) = 1 - \frac{2}{e^{2t} + 1}. \quad (5.4)$$

It is also straightforward to verify that for any given $\eta > 0$ sufficiently small, there exists a unique γ_η for γ , such that Eq. (5.1) for $\gamma = \gamma_\eta$ admits a heteroclinic solution from P^* to P , which we denote as $\ell_\eta^* = (a_\eta^*(t), b_\eta^*(t))$. We do not have an explicit formula for ℓ_η^* but at $\eta = 0$ we have

$$a_0^*(t) = \frac{4e^{2t}}{(e^{2t} + 1)^2}, \quad b_0^*(t) = \frac{2}{e^{2t} + 1} - 1. \quad (5.5)$$

In the rest of this section we assume that $\eta > 0$ is sufficiently small and $\gamma = \gamma_\eta$. Let us fix a value of η and set $\gamma = \gamma_\eta$. We now add a time-periodic perturbation to Eq. (5.1) to obtain the non-autonomous equation

$$\frac{dx}{dt} = 2xy - \eta(x + \gamma_\eta x^2) + \mu(y^2 - 1)^2 \sin \omega t, \quad \frac{dy}{dt} = 1 - 2x - y^2 \quad (5.6)$$

where μ is a parameter representing the magnitude of the perturbation and ω is the forcing frequency. Eq. (5.6) is the equation we study in this section.

5.2. Application of Theorems 2.1–2.4

First we compute the Melnikov functions. For $\mathcal{W}(\theta)$ we have

$$E_\ell(t) = (1, 0) \begin{pmatrix} 2b(t) - \eta & 0 \\ -2 & -2b(t) \end{pmatrix} \begin{pmatrix} 1 \\ 0 \end{pmatrix} = 2b(t) - \eta. \quad (5.7)$$

It then follows that

$$\begin{aligned} \mathcal{W}(\theta) &= \int_{-\infty}^{\infty} ((b(t))^2 - 1)^2 \sin \omega(t + \theta) e^{-\int_0^t E_\ell(s) ds} dt \\ &= \sqrt{J_c^2 + J_s^2} \sin(\omega\theta + \arctan(J_s(J_c)^{-1})), \end{aligned} \quad (5.8)$$

where

$$\begin{aligned}
J_c &= \int_{-\infty}^{\infty} ((b(t))^2 - 1)^2 e^{-\int_0^t (2b(s) - \eta) ds} \cos \omega t \, dt, \\
J_s &= \int_{-\infty}^{\infty} ((b(t))^2 - 1)^2 e^{-\int_0^t (2b(s) - \eta) ds} \sin \omega t \, dt.
\end{aligned} \tag{5.9}$$

For $\mathcal{W}^*(\theta)$, we have

$$E_{\ell^*}(t) = \frac{((b_\eta^*)'(t), -(a_\eta^*)'(t))}{((a_\eta^*)'(t))^2 + ((b_\eta^*)'(t))^2} \begin{pmatrix} 2b_\eta^*(t) - \eta(1 + 2\gamma a_\eta^*(t)) & 2a_\eta^*(t) \\ -2 & -2b_\eta^*(t) \end{pmatrix} \begin{pmatrix} (b_\eta^*)'(t) \\ -(a_\eta^*)'(t) \end{pmatrix}, \tag{5.10}$$

and it follows that

$$\begin{aligned}
\mathcal{W}^*(\theta) &= \int_{-\infty}^{\infty} \frac{(b_\eta^*)'(t)((b_\eta^*)^2(t) - 1)^2 \sin \omega(t + \theta)}{\sqrt{((a_\eta^*)'(t))^2 + ((b_\eta^*)'(t))^2}} e^{-\int_0^t E_{\ell^*}(s) ds} dt \\
&= \sqrt{(J_c^*)^2 + (J_s^*)^2} \sin(\omega\theta + \arctan(J_s^*(J_c^*)^{-1})),
\end{aligned} \tag{5.11}$$

where

$$\begin{aligned}
J_c^* &= \int_{-\infty}^{\infty} \frac{(b_\eta^*)'(t)((b_\eta^*)^2(t) - 1)^2}{\sqrt{((a_\eta^*)'(t))^2 + ((b_\eta^*)'(t))^2}} e^{-\int_0^t E_{\ell^*}(s) ds} \cos \omega t \, dt, \\
J_s^* &= \int_{-\infty}^{\infty} \frac{(b_\eta^*)'(t)((b_\eta^*)^2(t) - 1)^2}{\sqrt{((a_\eta^*)'(t))^2 + ((b_\eta^*)'(t))^2}} e^{-\int_0^t E_{\ell^*}(s) ds} \sin \omega t \, dt.
\end{aligned} \tag{5.12}$$

Lemma 5.1. *There exists an $\eta_0 > 0$ sufficiently small, such that for all positive $\eta < \eta_0$, we have $J_c^2 + J_s^2 \neq 0$, $(J_c^*)^2 + (J_s^*)^2 \neq 0$.*

Proof. It suffices to compute J_c , J_s , J_c^* , J_s^* at $\eta = 0$, for which all quantities involved are explicit. In fact, a direct computation yields that, for $\eta = 0$,

$$\begin{aligned}
J_c &= \frac{\pi e^{-\frac{1}{2}\omega\pi}}{60(1 - e^{-\omega\pi})} (\omega^5 + 20\omega^3 + 64\omega), & J_s &= 0; \\
J_c^* &= -\frac{\pi e^{-\frac{1}{2}\omega\pi}}{60(1 - e^{-\omega\pi})} (\omega^5 + 20\omega^3 + 64\omega), & J_s^* &= 0. \quad \square
\end{aligned}$$

We are now ready to apply Theorems 2.1–2.4 to Eq. (5.6). In the rest of our discussion, the parameters ω, η, γ are fixed in the following order: First we fix an $\omega \neq 0$; we then fix an irrational η sufficiently small, and let $\gamma = \gamma_\eta$ be such that the heteroclinic solution ℓ^* exists for the unperturbed equation (5.1). Let η be sufficiently small so that Lemma 5.1 holds.

Verification of (H1)–(H3). For (H1) we observe that $\alpha + \beta = -\eta < 0$, $\alpha^* + \beta^* = -\eta < 0$ for $\eta > 0$. To satisfy the non-resonance condition, it suffices to make η irrational. For (H2) we observe that

for Eq. (5.6), $P(x, y, t) = (1 - y^2)^2 \sin \omega t$, $Q(x, y) = 0$. (H3) follows directly from (5.8), (5.11) and Lemma 5.1.

Application of Theorems 2.1 and 2.2. First we arbitrarily fix a forcing frequency $\omega > 0$. We then fix a sufficiently small η that is irrational and let $\gamma = \gamma_\eta$. Let η be sufficiently small so that Lemma 5.1 holds. Then Theorems 2.1 and 2.2 apply to Eq. (5.6).

Application of Theorem 2.3. It is straightforward to verify that all critical points of

$$\mathcal{D}(\theta) = \theta - \frac{1}{\beta^*} \ln \mathcal{W}(\theta - C)$$

are non-degenerate for all C and all ω where $\mathcal{W}(\theta)$ is as in (5.8). This is sufficient for Theorem 2.3 to apply.

Application of Theorem 2.4. We prove that there exists an $\omega_0 > 0$ sufficiently large, so that for any given $\omega > \omega_0$, there exists an η_0 depending on ω , so that for any given irrational $0 < \eta < \eta_0$ and γ_η , there are infinitely many $\tilde{h} \rightarrow \infty$, so that the assumptions of Theorem 2.4 are satisfied.

We start our proof of this statement by observing that, for ω sufficiently large,

$$|J|, |J^*| = \mathcal{O}(\omega^{-2}) \quad (5.13)$$

where J, J^* be as in (2.12). This follows directly from (5.8) and (5.11).

Next, let $C, C^*, \mathcal{K}, \mathcal{K}^*$ be as in (2.8) and (2.11) respectively. We have

$$\begin{aligned} \mathcal{D}_h(\theta) &= \frac{h}{\beta^*} + \mathcal{K} + \theta - \frac{1}{\beta^*} \ln \sqrt{J_c^2 + J_s^2} \sin \omega(\theta - \psi), \\ \mathcal{D}_h^*(\theta) &= \frac{h}{\beta} + \mathcal{K}^* + \theta - \frac{1}{\beta} \ln \sqrt{(J_c^*)^2 + (J_s^*)^2} \sin \omega(\theta - \psi^*), \end{aligned}$$

where

$$\psi = C - \omega^{-1} \arctan J_s J_c^{-1}, \quad \psi^* = C^* - \omega^{-1} \arctan J_s^* (J_c^*)^{-1}.$$

We also have from (2.9),

$$I_- = \left(\psi - \frac{\pi}{\omega}, \psi \right), \quad I_-^* = \left(\psi^* - \frac{\pi}{\omega}, \psi^* \right)$$

where I_- and I_-^* are both treated as intervals in $S^1 = \mathbb{R}/(2\pi\omega^{-1}\mathbb{Z})$. (5.13) implies that, for ω sufficiently large, it suffices for us to prove

Lemma 5.2. *There exist infinitely many values of h , such that*

$$\mathcal{D}_h(\pi(2\omega)^{-1} + \psi) \in I_-^*, \quad \mathcal{D}_h^*(\pi(2\omega)^{-1} + \psi^*) \in I_-. \quad (5.14)$$

Proof. (5.14) holds if and only if there exists a pair of integers (m, n) such that

$$\frac{h}{\beta^*} - 2\pi\omega^{-1}n \in -\mathcal{K} - \pi(2\omega)^{-1} + \psi^* - \psi - \frac{1}{\beta^*} \ln \sqrt{J_c^2 + J_s^2} + \left(-\frac{\pi}{\omega}, 0\right), \quad (5.15)$$

$$\frac{h}{\beta} - 2\pi\omega^{-1}m \in -\mathcal{K}^* - \pi(2\omega)^{-1} + \psi - \psi^* - \frac{1}{\beta} \ln \sqrt{(J_c^*)^2 + (J_s^*)^2} + \left(-\frac{\pi}{\omega}, 0\right). \quad (5.16)$$

Direct computation yields that, at $\eta = 0$,

$$C = \frac{1}{4} \ln 20, \quad C^* = \frac{1}{2} \ln 2, \quad \mathcal{K} = \frac{1}{4} \ln 2000, \quad \mathcal{K}^* = \frac{1}{4} \ln 80,$$

from which it follows that, at $\eta = 0$,

$$-\mathcal{K} - \pi(2\omega)^{-1} + \psi - \psi^* = -\mathcal{K}^* - \pi(2\omega)^{-1} + \psi^* - \psi \pmod{2\pi\omega^{-1}}.$$

Here we also use the fact that $|J_c^*| = |J_c|$, $J_s = J_s^* = 0$ at $\eta = 0$. Therefore the two intervals at the right-hand side of (5.15) and (5.16) in $S^1 = (0, 2\pi\omega^{-1})$ overlap completely at $\eta = 0$. Since the size of both intervals is $\pi\omega^{-1}$, it then follows that, for $\eta > 0$ sufficiently small, they overlap in S^1 . Denote the intersection of these two intervals as \tilde{I} . Let n_0, m_0 be such that

$$\begin{aligned} -\mathcal{K} - 3\pi(2\omega)^{-1} + \psi - \psi^* - 2\pi n_0\omega^{-1} - \frac{1}{\beta^*} \ln \sqrt{J_c^2 + J_s^2} &\in (0, 2\pi\omega^{-1}), \\ -\mathcal{K}^* - 3\pi(2\omega)^{-1} + \psi^* - \psi - 2\pi m_0\omega^{-1} - \frac{1}{\beta} \ln \sqrt{J_c^2 + J_s^2} &\in (0, 2\pi\omega^{-1}). \end{aligned}$$

Then (5.15) and (5.16) hold if

$$\frac{h}{\beta^*} - 2\pi\omega^{-1}(n - n_0) \in \tilde{I}, \quad (5.17)$$

$$\frac{h}{\beta} - 2\pi\omega^{-1}(m - m_0) \in \tilde{I}. \quad (5.18)$$

We prove that there exist infinitely many h , each accompanied by a pair $(n(h), m(h))$, such that both (5.17) and (5.18) are fulfilled. Let (q_k, p_k) be such that

$$\frac{\beta}{\beta^*} = \frac{p_k}{q_k} + \mathcal{O}\left(\frac{1}{q_k^2}\right).$$

We let

$$n - n_0 = p_k, \quad m - m_0 = q_k, \quad h = 2\pi\omega^{-1}\beta^*p_k + \beta^*\theta_0$$

where $\theta_0 \in (0, 2\pi\omega^{-1})$ is the middle point of \tilde{I} . (5.17) is directly fulfilled by design. For (5.18), we observe that

$$\frac{h}{\beta} - 2\pi\omega^{-1}(m - m_0) = 2\pi\omega^{-1}\frac{\beta^*}{\beta}p_k - 2\pi\omega^{-1}q_k + \frac{\beta^*}{\beta}\theta_0 = \mathcal{O}\left(\frac{1}{q_k}\right) + \frac{\beta^*}{\beta}\theta_0 \in \tilde{I}$$

for all k sufficiently large. \square

Table 1
The values of η and γ_η .

η	1.000000000000	0.666666666666
γ_η	-1.288434637703	-1.266580375163

5.3. Numerical simulations

In this subsection we present a systematic numerical study of the periodically forced equation

$$\frac{dx}{dt} = 2xy - \eta(x + \gamma_\eta x^2) + \mu(y^2 - 1)^2 \sin 2\pi t, \quad \frac{dy}{dt} = 1 - 2x - y^2. \quad (5.19)$$

Our study is guided by the theory developed in the previous sections. Let Λ_μ be the heteroclinic tangle as defined at the end of Section 2.1 for Eq. (5.19). From the conclusions of Section 5.2 we know that

- (I) There are three major dynamical scenarios for Λ_μ competing in the μ -space. They are
 - (A) *Transient tangles* asserted by Theorem 2.4;
 - (B) *Tangles dominated by sinks* representing stable dynamics asserted by Theorem 2.2;
 - (C) *Hénon-like attractors* representing chaos asserted by Theorem 2.3.
- (II) As $\mu \rightarrow 0$, the dynamical behavior of the heteroclinic tangles are organized in a pattern determined by the unstable eigenvalues β and β^* .

Both (I) and (II) are instructive in numerical explorations. We can now tell comprehensively what to expect, and confirm these expectations in numerical simulations of Eq. (5.19) around the unperturbed heteroclinic loop.

5.3.1. Simulation procedure

The initial phase position (x_0, y_0) is always fixed at $x_0 = 0.05$, $y_0 = 0.05$. For the parameter η , simulations are performed for two specific values: $\eta = 1.0$ and $\eta = \frac{2}{3}$. We first integrate the unperturbed equation (by setting $\mu = 0$ in (5.19)) to find γ_η , the value of γ that admits a heteroclinic solution from $P^* = (0, 1)$ to $P = (0, -1)$. Because in our simulation μ reaches 10^{-8} in magnitude, we calculate the values of γ_η up to the precision of 10^{-12} . The values of η and γ_η are listed in Table 1.

Let the initial phase position (x_0, y_0) and the values of η and $\gamma = \gamma_\eta$ be fixed as above. Next we fix a value of μ . The range for μ is in between 10^{-3} to 10^{-8} . We then vary the initial time t_0 over $[0, T)$ where $T = 1$ is the forcing period for Eq. (5.19). Every t_0 now defines a solution, which we compute numerically by using the fourth order Runge–Kutta method. By Propositions 3.1 and 3.2, the dynamics of the heteroclinic tangle Λ_μ for a given value of μ is best reflected in the different behavior of the solutions over different initial times.

We use the following format in plotting a solution. Three plots, labelled as sub-figures (a), (b) and (c), are presented. See Fig. 6(a)–(c) and Fig. 7(a)–(c). We use (a) to plot $(x(kT), y(kT))$. This is to say that to plot (a) is to view the solution in the form of a discrete orbit of the time- T map. (b) is a plot for $(k, x(kT))$, the x -coordinate versus the time. (c) is the Fourier spectrum of $x(kT)$.

Technical restrictions imposed by the assumptions of the theorems are often disregarded in numerical simulations. $\eta = 1$ and $\frac{2}{3}$ are way out of the range that validate the theorems and they both defy the assumption that η is irrational. Our purpose is not to numerically confirm the conclusions the theorems asserted, but to use them as a guidance and a motivation to explore numerically the possibilities for the dynamics of the heteroclinic tangles of Eq. (5.19).

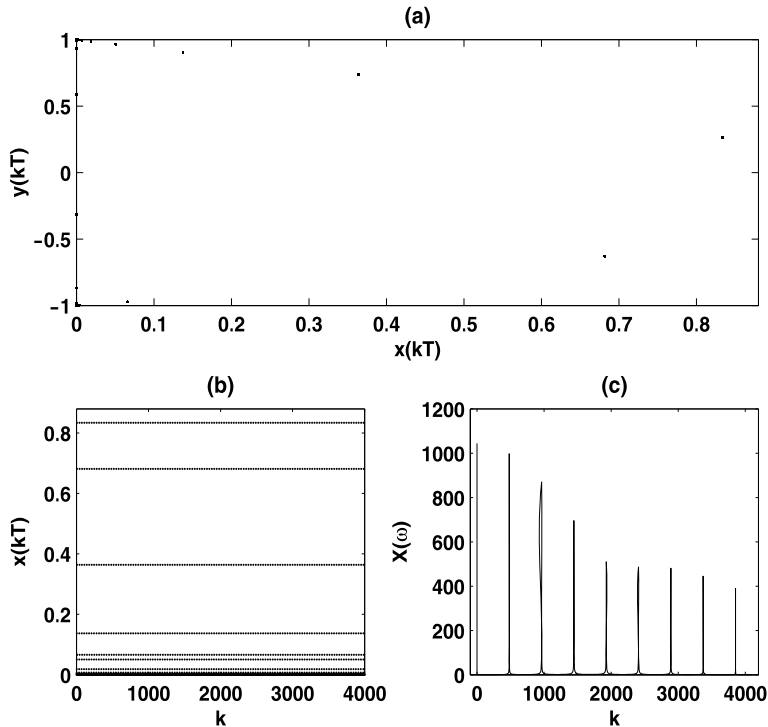


Fig. 6. Periodic sink with $\eta = 1$, $\mu = 3.5 \cdot 10^{-6}$, $t_0 = 0.4$.

5.3.2. Behavior of individual solutions

All solutions we integrate fall into one of the three categories as follows

(1) The solution quickly leaves the neighborhood of the unperturbed heteroclinic loop. In this case this solution does not catch anything directly observable inside of the heteroclinic tangle and there is nothing to plot.

(2) The solution stays forever close to the unperturbed heteroclinic loop, and the plots returned are as shown in Fig. 6. In this case the numerical integration catches a periodic sink inside of the heteroclinic tangle. Isolated dots shown in Fig. 6(a) represent a discrete periodic orbit for the time-T map. Horizontal lines in Fig. 6(b) illustrate that the discrete orbit plotted in (a) is indeed a periodic orbit.

(3) The solution again stays close to the unperturbed heteroclinic loop and the plots returned are as in Fig. 7. Fig. 7(a) is a plot of a Hénon-like attractor of Theorem 2.3, in which chaos is displayed around a periodic solution. The periodic pattern of the discrete orbit and the randomness of the x -coordinate are clearly illustrated in Fig. 7(b).

5.3.3. Three types of heteroclinic tangles

We fix a value of μ and varying t_0 over $[0, 1)$ with $\Delta t_0 = 0.001$. This is to say we integrate, numerically, one thousand solutions for a given μ value. Numerical simulations, for all values of μ , return one of the three types of heteroclinic tangles as follows.

(1)(A) (*Transient tangles*) In this case, all solutions leave the neighborhood of the heteroclinic loop of the unperturbed equation. This implies that the corresponding heteroclinic tangle contains no dynamical object that is directly observable. For this value of μ , the heteroclinic tangle is the type asserted by Theorem 2.4. We note that the attractive basin of a uniformly hyperbolic horseshoe is a set of Lebesgue measure zero therefore a horseshoe is not a directly observable object.

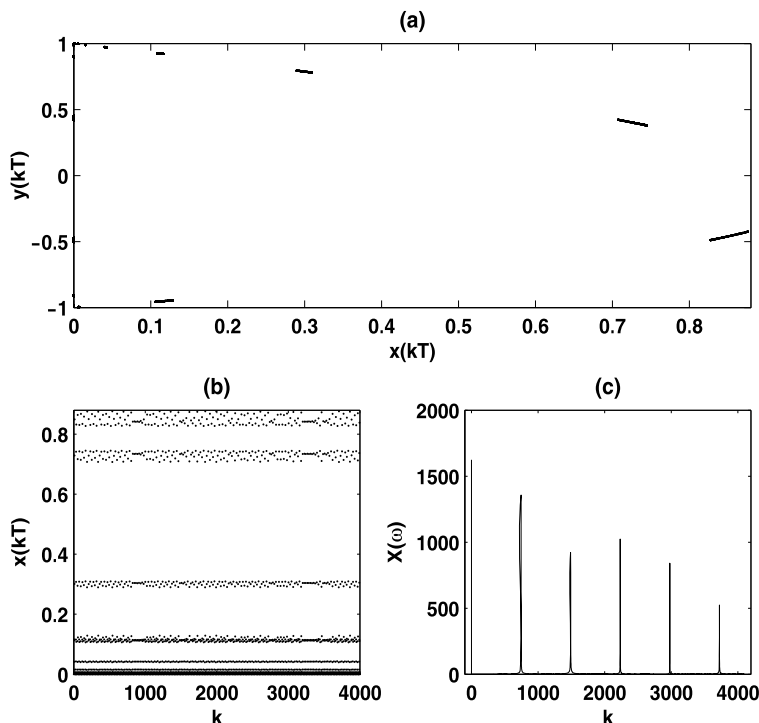


Fig. 7. Hénon-like attractor with $\eta = 1$, $\mu = 1.43 \cdot 10^{-3}$, $t_0 = 0.2$.

(I)(B) (*Tangles dominated by sinks*) In this case, there are values of t_0 , for which the corresponding solutions stay close to the unperturbed heteroclinic loop forever. When plotted, such solutions are all in the same category as that of Fig. 6. In this case we have a heteroclinic tangle dominated by periodic sinks representing stable dynamics.

(I)(C) (*Hénon-like attractors*) Again, solutions for some t_0 stay close to the unperturbed heteroclinic loop for all time, but the plots returned are the likes of Fig. 7. In this case we have a heteroclinic tangle with a Hénon-like attractor representing chaos in a directly observable form.

5.3.4. The quasi-periodic occurrence of dynamical behavior

For heteroclinic tangles, there are two intrinsic *multiplicative periods* induced by the two unstable eigenvalues β and β^* , and the occurrence of the three types of heteroclinic tangles is organized by the two working together. If β and β^* are rationally related, say, $\beta/\beta^* = m/n$, then there would be a repeating periodic pattern and the multiplicative period for μ would be $e^{\beta n T} = e^{\beta^* m T}$ where T is the forcing period. As the order of the resonance of β and β^* go higher, the multiplicative period would get larger and the repeating periodic pattern become more complicated. The periodicity of dynamical behavior would disappear as β and β^* become irrationally related.

To illustrate this pattern of dynamical behavior, we simulate using $\eta = 1$ and $\eta = 2/3$. In the case of $\eta = 1$, we have $\beta = 2$, $\beta^* = 1$. According to the theory, there is a repetitive pattern of dynamical behavior and the multiplicative period is $e^2 \approx 7.389$. Simulation results for $\eta = 1$ are tabulated in Table 2. The transitional values of μ , at which the heteroclinic tangles change from one type to another, are tabulated. The repetitive pattern in one multiplicative period, with the precision for μ initially set up to two effective digits, is

$$I(C), I(B), I(A), I(C), I(B), I(A), I(B), I(A).$$

Table 2

Multiplicative periodicity of dynamical behavior with $\eta = 1$ ($\eta = 1$, $\gamma = -1.288434637703$, theoretical ratio ≈ 7.389).

μ	Behavior type	Ratio
6.4E–03	I(C) (Hénon-like Attractors)	
6.3E–03	I(B) (Dominated by Sinks)	
6.2E–03	I(A) (Transient Tangle)	
3.9E–03	I(C) (Hénon-like Attractors)	
3.8E–03	I(B) (Dominated by Sinks)	
3.7E–03	I(A) (Transient Tangle)	
1.4E–03	I(B) (Dominated by Sinks)	
1.3E–03	I(A) (Transient Tangle)	
8.668E–04	I(C) (Hénon-like Attractors)	7.38
8.576E–04	I(B) (Dominated by Sinks)	7.35
8.470E–04	I(A) (Transient Tangle)	7.32
5.282E–04	I(C) (Hénon-like Attractors)	7.38
5.202E–04	I(B) (Dominated by Sinks)	7.30
5.137E–04	I(A) (Transient Tangle)	7.20
1.913E–04	I(B) (Dominated by Sinks)	7.32
1.890E–04	I(A) (Transient Tangle)	6.88
1.178E–04	I(C) (Hénon-like Attractors)	7.36
1.160E–04	I(B) (Dominated by Sinks)	7.39
1.146E–04	I(A) (Transient Tangle)	7.39
7.149E–05	I(C) (Hénon-like Attractors)	7.39
7.041E–05	I(B) (Dominated by Sinks)	7.39
6.953E–05	I(A) (Transient Tangle)	7.39
2.590E–05	I(B) (Dominated by Sinks)	7.39
2.558E–05	I(A) (Transient Tangle)	7.39
1.595E–05	I(C) (Hénon-like Attractors)	7.39
1.571E–05	I(B) (Dominated by Sinks)	7.38
1.551E–05	I(A) (Transient Tangle)	7.39
9.675E–06	I(C) (Hénon-like Attractors)	7.39
9.528E–06	I(B) (Dominated by Sinks)	7.39
9.410E–06	I(A) (Transient Tangle)	7.39
3.505E–06	I(B) (Dominated by Sinks)	7.39
3.462E–06	I(A) (Transient Tangle)	7.39
2.158E–06	I(C) (Hénon-like Attractors)	7.39
2.126E–06	I(B) (Dominated by Sinks)	7.39
2.099E–06	I(A) (Transient Tangle)	7.39
1.309E–06	I(C) (Hénon-like Attractors)	7.39
1.289E–06	I(B) (Dominated by Sinks)	7.39
1.273E–06	I(A) (Transient Tangle)	7.39
4.744E–07	I(B) (Dominated by Sinks)	7.39
4.685E–07	I(A) (Transient Tangle)	7.39

As shown in Table 2, this pattern repeats as we run the value of μ down to the magnitude of 10^{-7} . The ratios of the values of μ for the same position in this repetitive pattern in consecutive periods are calculated and they all appear reasonably close to $e^2 \approx 7.389$. In later periods, the precision for the value of μ are maintained up to four effective digits.

Table 3 is for $\eta = \frac{2}{3}$. In this case the theoretical value of the multiplicative period is $e^4 \approx 54.597$. Again, the transitional μ values and the corresponding type of heteroclinic tangles are tabulated. Since the order of resonance is now higher, the dynamical pattern inside one multiplicative period is more complicated. The repetitive pattern within one multiplicative period, with the precision for μ initially set up to two effective digits, is

$$I(A), I(B), I(A), I(C), I(A), I(C), I(B), I(A), I(B), I(A), I(B), I(A), I(B).$$

Table 3
Multiplicative periodicity of dynamical behavior with $\eta = \frac{2}{3}$ ($\eta = 0.666666666666$, $\gamma = -1.266580375163$, theoretical ratio ≈ 54.597).

μ	Behavior type	Ratio
5.8E−03	I(A) (Transient Tangle)	
3.1E−03	I(B) (Dominated by Sinks)	
2.9E−03	I(A) (Transient Tangle)	
1.6E−03	I(C) (Hénon-like Attractors)	
1.5E−03	I(A) (Transient Tangle)	
8.2E−04	I(C) (Hénon-like Attractors)	
8.1E−04	I(B) (Non-chaotic Tangle)	
7.9E−04	I(A) (Transient Tangle)	
4.2E−04	I(B) (Dominated by Sinks)	
4.0E−04	I(A) (Transient Tangle)	
2.1E−04	I(B) (Dominated by Sinks)	
2.0E−04	I(A) (Transient Tangle)	
1.1E−04	I(B) (Dominated by Sinks)	
1.070E−04	I(A) (Transient Tangle)	54.21
5.694E−05	I(B) (Dominated by Sinks)	54.44
5.494E−05	I(A) (Transient Tangle)	52.78
2.937E−05	I(C) (Hénon-like Attractors)	54.48
2.820E−05	I(A) (Transient Tangle)	53.19
1.512E−05	I(C) (Hénon-like Attractors)	54.23
1.500E−05	I(B) (Dominated by Sinks)	54.00
1.448E−05	I(A) (Transient Tangle)	54.56
7.702E−06	I(B) (Dominated by Sinks)	54.53
7.436E−06	I(A) (Transient Tangle)	53.79
3.954E−06	I(B) (Dominated by Sinks)	53.11
3.817E−06	I(A) (Transient Tangle)	52.40
2.030E−06	I(B) (Dominated by Sinks)	54.19
1.960E−06	I(A) (Transient Tangle)	54.59
1.042E−06	I(B) (Dominated by Sinks)	54.64
1.006E−06	I(A) (Transient Tangle)	54.61
5.380E−07	I(C) (Hénon-like Attractors)	54.59
5.166E−07	I(A) (Transient Tangle)	54.59
2.769E−07	I(C) (Hénon-like Attractors)	54.60
2.741E−07	I(B) (Dominated by Sinks)	54.72
2.652E−07	I(A) (Transient Tangle)	54.60
1.410E−07	I(B) (Dominated by Sinks)	54.62
1.361E−07	I(A) (Transient Tangle)	54.64
7.228E−08	I(B) (Dominated by Sinks)	54.70
6.990E−08	I(A) (Transient Tangle)	54.61
3.707E−08	I(B) (Dominated by Sinks)	54.76

This pattern again repeats periodically, as shown in Table 3, as we run the value of μ down to the magnitude of 10^{-8} . The ratios of the values of μ for the same position in this repetitive pattern in consecutive periods are again calculated and they all appear reasonably close to $e^4 \approx 54.597$. In later periods, the precision for the values of μ is again maintained up to four effective digits. Because the order of non-resonance is higher in this case, the multiplicative period and the string for the pattern of dynamical behavior in one period are both longer.

We caution that, in theory, the dynamical pattern inside each of the multiplicative period is always infinitely complicated. In simulations, however, there are only finitely many possibilities and the level of complexity showing up depends on the level of precision one decides to adopt. Therefore the comparisons in complexity we talked above are comparisons made by using the same level of precision for μ .

We also caution that the transitional values of μ presented in Tables 2 and 3 depend sensitively not only on the adopted level of precision of the parameters, but also on the step size of the numerical integration and even the way the program is written and compiled. The μ values presented in Tables 1–3 would be all slightly off if the reader uses his/her own program. What is always repeatable,

however, is the three types of heteroclinic tangles and the periodic patterns shown in Tables 2 and 3. Since we are simulating a delicate dynamical situation of infinitesimal precision, this is completely expected and is indeed a nice character of the theory.

Appendix A. Derivation of the separatrix map

In this appendix we derive the formula for $\mathcal{R} : \Sigma \rightarrow \Sigma^*$ in Proposition 3.1. The Poincaré sections $\Sigma, \Gamma, \Sigma_*, \Gamma_*$ are introduced in precise terms by using the linearized coordinates around P and P^* in Section A.1. Normal forms around the heteroclinic solutions are derived in Section A.3. Issues related to coordinate conversion are discussed in detail in Section A.4. Derivations for the formula $\mathcal{R}^* : \Sigma^* \rightarrow \Sigma$ in Proposition 3.2 are similar.

A.1. The Poincaré sections

We start with the linearization of Eq. (2.3) on $B_\varepsilon(P)$, the ε -neighborhood of the fixed point $P = (q, p)$. Let J be the Jacobian matrix of Eq. (2.1) at P , $\alpha < 0 < \beta$ be the eigenvalues of J and let ξ_α, ξ_β be their corresponding eigenvectors. We say that α and β are non-resonant up to order N_0 if there exist no integers $m, n > 0$, $m + n \leq N_0$, so that

$$m\alpha + n\beta = 0.$$

We introduce a coordinate change $\mathcal{L}_\mu : (x, y) \rightarrow (X, Y)$ by letting

$$\begin{pmatrix} x - q \\ y - p \end{pmatrix} = M \begin{pmatrix} X \\ Y \end{pmatrix} + \begin{pmatrix} F(X, Y) \\ G(X, Y) \end{pmatrix} + \mu \begin{pmatrix} \tilde{F}(X, Y, \theta) \\ \tilde{G}(X, Y, \theta) \end{pmatrix} \quad (\text{A.1})$$

where M is the two-by-two matrix taking ξ_α, ξ_β as its two columns, and we have

$$M^{-1} J M = \begin{pmatrix} \alpha & 0 \\ 0 & \beta \end{pmatrix};$$

$F(X, Y), G(X, Y), \tilde{F}(X, Y, \theta), \tilde{G}(X, Y, \theta)$ are terms of order at least two in (X, Y) at $(0, 0)$ defined on $|(X, Y)| < \|M^{-1}\|\varepsilon$, and there exists a constant K independent of ε and μ such that their C^r -norms in X, Y, θ are $< K$. Recall that $r > 3$ is the desired smoothness for the separatrix map. We have

Proposition A.1. *There exists an $N_0 > 0$ depending on r , such that if we assume that $f(x, y), g(x, y), P(x, y, t), Q(x, y, t)$ are C^{N_0} and α, β are non-resonant up to degree N_0 , then there exists a change of coordinates $(x, y) \rightarrow (X, Y)$ as in (A.1), such that it transforms Eq. (2.3) to the linear equation*

$$\frac{dX}{dt} = \alpha X, \quad \frac{dY}{dt} = \beta Y, \quad \frac{d\theta}{dt} = 1$$

on $|(X, Y)| < \|M^{-1}\|\varepsilon$ provided that $\mu, \varepsilon, \mu \ll \varepsilon$, are both sufficiently small.

We note that the assumptions of this proposition are fulfilled by the assumption (H1).

Poincaré sections Σ and Γ . Let $(0, A)$ be such that $\mathcal{L}_0^{-1}(0, A) = \ell(-L_-)$. We have $A \approx \frac{1}{2}\varepsilon$. We define Σ in the space of (X, Y, θ) by letting

$$\Sigma = \{(X, Y, \theta) : |X| < \mu, Y = A, \theta \in S^1\}.$$

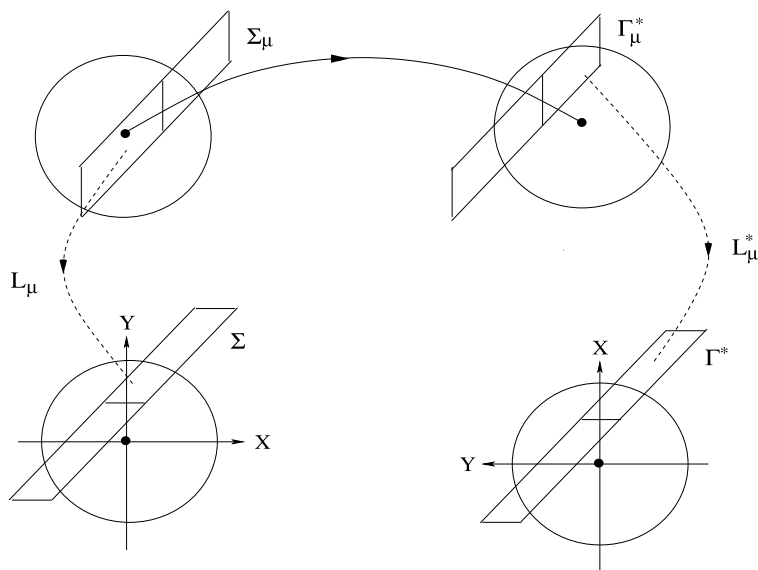


Fig. 8. The Poincaré sections.

Similarly, let $(B, 0)$ be such that $\mathcal{L}_0^{-1}(B, 0) = \ell^*(L_+^*)$. We have $B \approx \frac{1}{2}\varepsilon$. We define Γ in the space of (X, Y, θ) by letting

$$\Gamma = \{(X, Y, \theta): X = B, |Y| = K_1(\varepsilon)\mu, \theta \in S^1\},$$

where $K_1(\varepsilon)$ is a constant independent of μ , the value of which we will define in precise terms momentarily. We denote the images of Σ and Γ in the space of (x, y, θ) under \mathcal{L}_μ^{-1} as Σ_μ and Γ_μ respectively. This is to say that

$$\Sigma_\mu = \mathcal{L}_\mu^{-1}\Sigma, \quad \Gamma_\mu = \mathcal{L}_\mu^{-1}\Gamma.$$

See Fig. 8.

In completely similar terms, we assume that α^* and β^* are non-resonant up to order N_0 and we linearize Eq. (2.3) on $B_{\varepsilon^*}(P^*)$ by using a coordinate transformation $\mathcal{L}_\mu^*: (x, y) \rightarrow (X, Y)$ in the form of

$$\begin{pmatrix} x - q^* \\ y - p^* \end{pmatrix} = M^* \begin{pmatrix} X \\ Y \end{pmatrix} + \begin{pmatrix} F^*(X, Y) \\ G^*(X, Y) \end{pmatrix} + \mu \begin{pmatrix} \tilde{F}^*(X, Y, \theta) \\ \tilde{G}^*(X, Y, \theta) \end{pmatrix}. \quad (\text{A.2})$$

Let A^* be such that $(\mathcal{L}_0^*)^{-1}(0, A^*) = \ell^*(-L_-^*)$ and B^* be such that $(\mathcal{L}_0^*)^{-1}(B^*, 0) = \ell(L_+)$. Σ^* , Σ_μ^* , Γ^* , Γ_μ^* are defined by letting

$$\Sigma^* = \{(X, Y, \theta): |X| < \mu, Y = A^*, \theta \in S^1\}; \quad \Sigma_\mu^* = (\mathcal{L}_\mu^*)^{-1}\Sigma^*$$

and

$$\Gamma^* = \{(X, Y, \theta): X = B^*, |Y| = K_1^*(\varepsilon)\mu, \theta \in S^1\}, \quad \Gamma_\mu^* = (\mathcal{L}_\mu^*)^{-1}\Gamma^*.$$

Let $\mathcal{M} : \Sigma_\mu \rightarrow \Gamma_\mu^*$ be induced by the solutions of Eq. (2.3) and $\mathcal{N}^* : \Gamma^* \rightarrow \Sigma^*$ be induced by the linearized equation

$$\frac{dX}{dt} = \alpha^* X, \quad \frac{dY}{dt} = \beta^* Y, \quad \frac{d\theta}{dt} = 1 \quad (\text{A.3})$$

on $B_{\varepsilon^*}(P^*)$. Our objective here is to derive a formula for the map $\mathcal{R} : \Sigma \rightarrow \Sigma^*$ where

$$\mathcal{R} = \mathcal{N}^* \circ \mathcal{L}_\mu^* \circ \mathcal{M} \circ \mathcal{L}_\mu^{-1}.$$

A.2. The derivation of \mathcal{N}^*

A formula for $\mathcal{N}^* : \Gamma^* \rightarrow \Sigma^*$ induced by the linear equation (A.3) is straightforward. Since we have $X = B^*$ on Γ^* , a point on Γ^* is represented by a pair (Y, θ) . Similarly, a point on Σ^* is represented by a pair (X, θ) because $Y = A^*$ on Σ^* . We also re-scale the variables (X, Y) by letting

$$\mathbb{X} = \mu^{-1} X, \quad \mathbb{Y} = \mu^{-1} Y. \quad (\text{A.4})$$

A point on Γ^* is represented by a pair (\mathbb{Y}, θ) and a point on Σ^* is represented by a pair (\mathbb{X}, θ) . With these coordinates, we write $(\hat{\mathbb{X}}, \hat{\theta}) = \mathcal{N}^*(\mathbb{Y}, \theta)$. We have

Lemma A.1. For $(\hat{\mathbb{X}}, \hat{\theta}) = \mathcal{N}^*(\mathbb{Y}, \theta)$,

$$\hat{\theta} = \theta + \frac{1}{\beta^*} \ln(\mu^{-1} A^*) - \frac{1}{\beta^*} \ln \mathbb{Y}; \quad \hat{\mathbb{X}} = B^* A^{*\frac{\alpha^*}{\beta^*}} \mu^{-\frac{\alpha^*}{\beta^*}-1} \mathbb{Y}^{-\frac{\alpha^*}{\beta^*}}.$$

Proof. From solving

$$\hat{\mathbb{X}} = \mu^{-1} B^* e^{\alpha^*(\hat{\theta}-\theta)}, \quad \mu^{-1} A^* = \mathbb{Y} e^{\beta^*(\hat{\theta}-\theta)},$$

the conclusion of this lemma directly follows. \square

A.3. Normal form around heteroclinic solutions

To derive a formula for $\mathcal{M} : \Sigma_\mu \rightarrow \Gamma_\mu^*$, we work in a small neighborhood of size $\mathcal{O}(\mu)$ around the heteroclinic solution ℓ in (x, y, θ) -space, which we denote as D . We let

$$D = \{(x, y) : |(x, y) - \ell(t)| < K_1(\varepsilon)\mu, t \in (-2L_-, 2L_+)\}, \quad \mathcal{D} = D \times S^1.$$

First we introduce a coordinate change from (x, y) to (s, z) on D as follows. Regard the heteroclinic solution ℓ as a parameterized curve in the (x, y) -plane, and the time t in the solution formula $\ell(t)$ as the parameter. We use s to write $\ell(s)$ to indicate that s is a new phase variable, not the time. On D , we let (s, z) be such that

$$(x, y) = \ell(s) + \tau_\ell^\perp(s)z. \quad (\text{A.5})$$

We recall that $\ell(s) = (a(s), b(s))$ where $(a(t), b(t))$ satisfies Eq. (2.1); $\tau_\ell(s) = (u(s), v(s))$ where

$$u(s) = |(a'(s), b'(s))|^{-1} a'(s), \quad v(s) = |(a'(s), b'(s))|^{-1} b'(s);$$

and $\tau_\ell^\perp(s) = (v(s), -u(s))$. Differentiating with respect to t on both sides of (A.5), we obtain

$$\left(\frac{d\ell(s)}{ds} + z \frac{d\tau_\ell^\perp(s)}{ds} \right) \frac{ds}{dt} + \tau_\ell^\perp(s) \frac{dz}{dt} = (F(s, z, \theta, \mu), G(s, z, \theta, \mu)) \quad (\text{A.6})$$

where

$$\begin{aligned} F(s, z, \theta, \mu) &= f(\ell(s) + \tau_\ell^\perp(s)z) + \mu P(\ell(s) + \tau_\ell^\perp(s)z, \theta), \\ G(s, z, \theta, \mu) &= g(\ell(s) + \tau_\ell^\perp(s)z) + \mu Q(\ell(s) + \tau_\ell^\perp(s)z, \theta). \end{aligned} \quad (\text{A.7})$$

From (A.6) it follows that

$$\begin{aligned} \frac{ds}{dt} &= \frac{\tau_\ell(s) \cdot (F(s, z, \theta, \mu), G(s, z, \theta, \mu))}{\tau_\ell(s) \cdot \left(\frac{d\ell(s)}{ds} + z \frac{d\tau_\ell^\perp(s)}{ds} \right)}, \\ \frac{dz}{dt} &= \tau_\ell^\perp(s) \cdot (F(s, z, \theta, \mu), G(s, z, \theta, \mu)). \end{aligned} \quad (\text{A.8})$$

As a final step, we re-scale z by letting

$$Z = \mu^{-1}z. \quad (\text{A.9})$$

We write Eq. (A.8) in variables (s, Z) as

$$\begin{aligned} \frac{ds}{dt} &= \frac{\tau_\ell(s) \cdot (F(s, \mu Z, \theta, \mu), G(s, \mu Z, \theta, \mu))}{\tau_\ell(s) \cdot \left(\frac{d\ell(s)}{ds} + \mu Z \frac{d\tau_\ell^\perp(s)}{ds} \right)}, \\ \frac{dZ}{dt} &= \mu^{-1} \tau_\ell^\perp(s) \cdot (F(s, \mu Z, \theta, \mu), G(s, \mu Z, \theta, \mu)). \end{aligned} \quad (\text{A.10})$$

Therefore on the domain defined by

$$\mathcal{D} = \{|Z| < K_1(\varepsilon), s \in (-2L_-, 2L_+), \theta \in S^1\}$$

we have

$$\begin{aligned} \frac{ds}{dt} &= 1 + \mathcal{O}_{s,Z,\theta,h}(\mu), \\ \frac{dZ}{dt} &= E_\ell(s)Z + (P(\ell(s), \theta), Q(\ell(s), \theta)) \cdot \tau_\ell^\perp(s) + \mathcal{O}_{s,Z,\theta,h}(\mu) \end{aligned} \quad (\text{A.11})$$

where

$$E_\ell(s) = \tau_\ell^\perp(s) \begin{pmatrix} \partial_x f(\ell(s)) & \partial_y f(\ell(s)) \\ \partial_x g(\ell(s)) & \partial_y g(\ell(s)) \end{pmatrix} \tilde{\tau}_\ell^\perp(s),$$

is as in (2.5).

A.4. Conversion of coordinates

The variables $(\mathbb{X}, \mathbb{Y}, \theta)$ and (s, Z, θ) are related by the coordinate transforms (A.1), (A.5) and the re-scales (A.4), (A.9). A point in Σ is represented by a pair (\mathbb{X}, θ) and \mathbb{Y} is such that $\mathbb{Y} = \mu^{-1}A$. A point in Σ_μ is also represented by a pair (Z, θ) , but the value of the third coordinate s is now a dependent on Z and θ . We start with a simple claim on the function $s = s(Z, \theta)$ that defines Σ_μ .

Lemma A.2. For $(s, Z, \theta) \in \Sigma_\mu$, we have $s = -L_- + \mathcal{O}_{Z, \theta, h}(\mu)$.

Proof. From (A.1) and (A.5), we have on Σ_μ ,

$$\ell(s) - P + \tau_\ell^\perp(s)z = M \begin{pmatrix} X \\ A \end{pmatrix} + \begin{pmatrix} F(X, A) \\ G(X, A) \end{pmatrix} + \mu \begin{pmatrix} \tilde{F}(X, A, \theta) \\ \tilde{G}(X, A, \theta) \end{pmatrix}.$$

We also have by definition,

$$\ell(-L_-) - P = M \begin{pmatrix} 0 \\ A \end{pmatrix} + \begin{pmatrix} F(0, A) \\ G(0, A) \end{pmatrix}.$$

By combining the two above we obtain

$$\ell(s) - \ell(-L_-) + \tau_\ell^\perp(s)z = M \begin{pmatrix} X \\ 0 \end{pmatrix} + \begin{pmatrix} F(X, A) - F(0, A) \\ G(X, A) - G(0, A) \end{pmatrix} + \mu \begin{pmatrix} \tilde{F}(X, A, \theta) \\ \tilde{G}(X, A, \theta) \end{pmatrix}. \quad (\text{A.12})$$

Let

$$\begin{pmatrix} W_1 \\ W_2 \end{pmatrix} = M^{-1}(\ell(s) - \ell(-L_-) + \tau_\ell^\perp(s)z) - \mu M^{-1} \begin{pmatrix} \tilde{F}(0, A, \theta) \\ \tilde{G}(0, A, \theta) \end{pmatrix}. \quad (\text{A.13})$$

We have from (A.12)

$$\begin{pmatrix} W_1 \\ W_2 \end{pmatrix} = \begin{pmatrix} X \\ 0 \end{pmatrix} + M^{-1} \begin{pmatrix} F(X, A) - F(0, A) \\ G(X, A) - G(0, A) \end{pmatrix} + \mu M^{-1} \begin{pmatrix} \tilde{F}(X, A, \theta) - \tilde{F}(0, A, \theta) \\ \tilde{G}(X, A, \theta) - \tilde{G}(0, A, \theta) \end{pmatrix}$$

which we rewrite as

$$\begin{aligned} W_1 &= (1 + \mathcal{O}(\varepsilon) + \mu[\mathcal{O}_\theta(1) + \mathcal{O}_{\theta, h}(\mu)])X + [\mathcal{O}_{X, \theta}(1) + \mathcal{O}_{X, \theta, h}(\mu)]X^2, \\ W_2 &= (\mathcal{O}(\varepsilon) + \mu[\mathcal{O}_\theta(1) + \mathcal{O}_{\theta, h}(\mu)])X + [\mathcal{O}_{X, \theta}(1) + \mathcal{O}_{X, \theta, h}(\mu)]X^2. \end{aligned} \quad (\text{A.14})$$

We first obtain

$$X = (1 + \mathcal{O}(\varepsilon) + \mu[\mathcal{O}_\theta(1) + \mathcal{O}_{\theta, h}(\mu)])W_1 + [\mathcal{O}_{W_1, \theta}(1) + \mathcal{O}_{W_1, \theta, h}(\mu)]W_1^2 \quad (\text{A.15})$$

by inverting the first line in (A.14). We then substitute it into the second line in (A.14) to obtain

$$W_2 = (\mathcal{O}(\varepsilon) + \mu[\mathcal{O}_\theta(1) + \mathcal{O}_{\theta, h}(\mu)])W_1 + [\mathcal{O}_{W_1, \theta}(1) + \mathcal{O}_{W_1, \theta, h}(\mu)]W_1^2 \quad (\text{A.16})$$

where W_1, W_2 as functions of s, Z, θ are defined by (A.13). Recall that ξ_α and ξ_β are the two eigenvectors of the Jacobian matrix J of Eq. (2.1) at $P = (q, p)$, and M is the two-by-two matrix

defined by ξ_α and ξ_β as its two columns. It follows that M^{-1} is the two-by-two matrix defined by ξ_β^\perp and $-\xi_\alpha^\perp$ as its two rows, divided also by $\det(M)$. We have

$$\begin{aligned} W_1 &= \frac{1}{\det(M)} \xi_\beta^\perp \cdot \left(\ell(s) - \ell(-L_-) + \mu \tau_\ell^\perp(s) Z - \mu \begin{pmatrix} \tilde{F}(0, A, \theta) \\ \tilde{G}(0, A, \theta) \end{pmatrix} \right), \\ W_2 &= \frac{-1}{\det(M)} \xi_\alpha^\perp \cdot \left(\ell(s) - \ell(-L_-) + \mu \tau_\ell^\perp(s) Z - \mu \begin{pmatrix} \tilde{F}(0, A, \theta) \\ \tilde{G}(0, A, \theta) \end{pmatrix} \right). \end{aligned} \quad (\text{A.17})$$

Let $\eta = s + L_-$. We rewrite W_1 and W_2 as

$$\begin{aligned} W_1 &= \frac{1}{\det(M)} \xi_\beta^\perp \cdot (|\ell'(-L_-)| \tau_\ell(-L_-) \eta + \mathcal{O}_\eta(1) \eta^2 + \mathcal{O}_{\eta, Z, \theta, h}(\mu)), \\ W_2 &= \frac{-1}{\det(M)} \xi_\alpha^\perp \cdot (|\ell'(-L_-)| \tau_\ell(-L_-) \eta + \mathcal{O}_\eta(1) \eta^2 + \mathcal{O}_{\eta, Z, \theta, h}(\mu)). \end{aligned}$$

Substituting into (A.16), we obtain

$$-(\xi_\alpha^\perp + \mathcal{O}(\varepsilon) \xi_\beta^\perp) \cdot \tau_\ell(-L_-) |\ell'(-L_-)| \eta + \mathcal{O}_{\eta, Z, \theta, h}(1) \eta^2 = \mathcal{O}_{\eta, Z, \theta, h}(\mu).$$

Note that we have

$$(\xi_\alpha^\perp + \mathcal{O}(\varepsilon) \xi_\beta^\perp) \cdot \tau_\ell(-L_-) |\ell'(-L_-)| \approx |\ell'(-L_-)| |\xi_\alpha^\perp \cdot \xi_\beta| \gg \mathcal{O}(\mu)$$

where the fact that $\tau_\ell(-L_-) \approx \xi_\beta$ is used. It then follows that $\eta = \mathcal{O}_{Z, \theta, h}(\mu)$. \square

We also need the following refinement of Lemma A.2

Lemma A.3. We have for (s, Z, θ) on Σ_μ ,

$$s + L_- = -\mu \frac{(\xi_\alpha^\perp \cdot \tau_\ell^\perp(-L_-) + \mathcal{O}(\varepsilon) \xi_\beta^\perp \cdot \tau_\ell^\perp(-L_-)) Z + \mathcal{O}_\theta(1)}{|\ell'(-L_-)| (\xi_\alpha^\perp \cdot \tau_\ell(-L_-) + \mathcal{O}(\varepsilon) \xi_\beta^\perp \cdot \tau_\ell(-L_-))} + \mathcal{O}_{Z, \theta, h}(\mu^2).$$

Proof. It suffices for us to drop all terms that are $\mathcal{O}_{Z, \theta, h}(\mu^2)$ in Eq. (A.16) by using (A.17) to solve for $s + L_-$. Note that it is important that we can use

$$\eta = s + L_- = \mathcal{O}_{Z, \theta, h}(\mu).$$

With terms of $\mathcal{O}_{Z, \theta, h}(\mu^2)$ all dropped out, (A.16) becomes

$$\eta = -\mu \frac{(\xi_\alpha^\perp \cdot \tau_\ell^\perp(-L_-) + \mathcal{O}(\varepsilon) \xi_\beta^\perp \cdot \tau_\ell^\perp(-L_-)) Z + \mathcal{O}_\theta(1)}{|\ell'(-L_-)| (\xi_\alpha^\perp \cdot \tau_\ell(-L_-) + \mathcal{O}(\varepsilon) \xi_\beta^\perp \cdot \tau_\ell(-L_-))}$$

from which Lemma A.3 follows directly. \square

We finally have the following on $\mathcal{L}_\mu^{-1} : \Sigma \rightarrow \Sigma_\mu$.

Lemma A.4. For $(\mathbb{X}, \theta) \in \Sigma$, let $(s, Z, \theta) = \mathcal{L}_\mu^{-1}(\mathbb{X}, \theta)$. Then we have

$$\mathbb{X} = \frac{1 + \mathcal{O}(\varepsilon)}{\xi_\alpha \cdot \xi_\beta^\perp} Z + \mathcal{O}_\theta(1) + \mathcal{O}_{Z, \theta, h}(\mu).$$

Proof. This lemma follows directly from (A.15) and (A.17) with the help of Lemma A.3. First from (A.17) we have

$$\begin{aligned} W_1 &= \frac{1}{\det(M)} \xi_\beta^\perp \cdot (\ell'(-L_-)(s + L_-) + \mu \tau_\ell^\perp(-L_-)Z + \mu \mathcal{O}_\theta(1) + \mathcal{O}_{Z, \theta, h}(\mu^2)) \\ &= \frac{\mu}{\det(M)} \xi_\beta^\perp \cdot \left(\tau_\ell(-L_-) \frac{(\xi_\alpha^\perp \cdot \tau_\ell^\perp(-L_-) + \mathcal{O}(\varepsilon) \xi_\beta^\perp \cdot \tau_\ell^\perp(-L_-))Z + \mathcal{O}_\theta(1)}{\xi_\alpha^\perp \cdot \tau_\ell(-L_-) + \mathcal{O}(\varepsilon) \xi_\beta^\perp \cdot \tau_\ell(-L_-)} + \tau_\ell^\perp(-L_-)Z \right) \\ &\quad + \mu \mathcal{O}_\theta(1) + \mathcal{O}_{Z, \theta, h}(\mu^2) \\ &= \frac{\mu}{\det(M)} (1 + \mathcal{O}(\varepsilon))Z + \mu \mathcal{O}_\theta(1) + \mathcal{O}_{Z, \theta, h}(\mu^2) \end{aligned}$$

where Lemma A.3 is used for the second equality. Substituting into (A.15), we obtain

$$\mathbb{X} = \frac{1}{\det(M)} (1 + \mathcal{O}(\varepsilon))Z + \mathcal{O}_\theta(1) + \mathcal{O}_{Z, \theta, h}(\mu).$$

We also note that $\det(M) = \xi_\alpha \cdot \xi_\beta^\perp$. \square

In completely symmetric forms, we have similar results for Σ^* , Γ and Γ^* . These results are summarized in the following two propositions.

Proposition A.2. (a) Use (\mathbb{X}, θ) to represent a point on Σ and let $(s, Z, \theta) = \mathcal{L}_\mu^{-1}(\mathbb{X}, \theta)$. We have $s = -L_- + \mathcal{O}_{Z, \theta, h}(\mu)$ and

$$\mathbb{X} = \frac{1 + \mathcal{O}(\varepsilon)}{\xi_\alpha \cdot \xi_\beta^\perp} Z + \mathcal{O}_\theta(1) + \mathcal{O}_{Z, \theta, h}(\mu).$$

(b) Use (\mathbb{Y}, θ) to represent a point on Γ , and let $(s, Z, \theta) = \mathcal{L}_\mu^{-1}(\mathbb{Y}, \theta)$. We have $s = L_+^* + \mathcal{O}_{Z, \theta, h}(\mu)$ and

$$\mathbb{Y} = \frac{1 + \mathcal{O}(\varepsilon)}{\xi_\alpha \cdot \xi_\beta^\perp} Z + \mathcal{O}_\theta(1) + \mathcal{O}_{Z, \theta, h}(\mu).$$

Proposition A.3. (a) Use (\mathbb{X}, θ) to represent a point on Σ^* and let $(s, Z, \theta) = (\mathcal{L}_\mu^*)^{-1}(\mathbb{X}, \theta)$. We have $s = -L_-^* + \mathcal{O}_{Z, \theta, h}(\mu)$ and

$$\mathbb{X} = \frac{1 + \mathcal{O}(\varepsilon^*)}{\xi_{\alpha^*} \cdot \xi_{\beta^*}^\perp} Z + \mathcal{O}_\theta(1) + \mathcal{O}_{Z, \theta, h}(\mu).$$

(b) Use (\mathbb{Y}, θ) to represent a point on Γ^* , and let $(s, Z, \theta) = (\mathcal{L}_\mu^*)^{-1}(\mathbb{Y}, \theta)$. We have $s = L_+ + \mathcal{O}_{Z, \theta, h}(\mu)$ and

$$\mathbb{Y} = \frac{1 + \mathcal{O}(\varepsilon^*)}{\xi_{\alpha^*} \cdot \xi_{\beta^*}^\perp} Z + \mathcal{O}_\theta(1) + \mathcal{O}_{Z, \theta, h}(\mu).$$

Proposition A.2(a) is Lemmas A.2 and A.4. Proposition A.2(b) and Proposition A.3(a), (b) are parallel to Proposition A.2(a) and the proofs are all similar.

A.5. Derivation of $\mathcal{M} : \Sigma_\mu \rightarrow \Gamma_\mu^*$

We use (s, Z, θ) as the phase variables and the normal form (A.11) to derive a formula for $\mathcal{M} : \Sigma_\mu \rightarrow \Gamma_\mu^*$.

Lemma A.5. For $(Z, \theta) \in \Sigma_\mu$, let $(\tilde{Z}, \tilde{\theta})$ be such that $(\tilde{Z}, \tilde{\theta}) = \mathcal{M}(Z, \theta)$. We have

$$\begin{aligned}\tilde{Z} &= M_+ \mathcal{W}_{L_-, L_+}(\theta + L_-) + M_+ M_- Z + \mathcal{O}_{Z, \theta, h}(\mu), \\ \tilde{\theta} &= \theta + L_+ + L_- + \mathcal{O}_{Z, \theta, h}(\mu)\end{aligned}\quad (\text{A.18})$$

where

$$\begin{aligned}M_+ &= e^{\int_0^{L_+} E_\ell(s) ds}, \quad M_- = e^{\int_{-L_-}^0 E_\ell(s) ds}; \\ \mathcal{W}_{L_-, L_+}(\theta) &= \int_{-L_-}^{L_+} [(P(\ell(t), t + \theta), Q(\ell(t), t + \theta)) \cdot \tau_{\ell(t)}^\perp] e^{-\int_0^t E_\ell(s) ds} dt;\end{aligned}\quad (\text{A.19})$$

and

$$E_\ell(t) = \tau_{\ell(t)}^\perp \begin{pmatrix} \partial_x f(\ell(t)) & \partial_y f(\ell(t)) \\ \partial_x g(\ell(t)) & \partial_y g(\ell(t)) \end{pmatrix} \tilde{\tau}_{\ell(t)}^\perp. \quad (\text{A.20})$$

Proof. The formula for $\tilde{Z}, \tilde{\theta}$ in this lemma follows directly from Eq. (A.11) and the fact that $s = -L_- + \mathcal{O}_{Z, \theta, h}(\mu)$ on Σ_μ , $s = L_+ + \mathcal{O}_{Z, \theta, h}(\mu)$ on Γ_μ^* . We also note that, in order for all solutions starting from Σ_μ to stay inside of D , it suffices to let

$$K_1(\varepsilon) = \sup_{\theta \in S^1, \tau \in [-2L_-, 2L_+]} |\mathcal{W}_{L_-, \tau}(\theta)| + M_+ M_-$$

where $\mathcal{W}_{L_-, \tau}(\theta)$ is defined by replacing the upper bound L_+ of the integral for $\mathcal{W}_{L_-, L_+}(\theta)$ by τ . This is the value of $K_1(\varepsilon)$ that defines D . \square

Proof of Proposition 3.1. The formula as stated in Proposition 3.1 is now obtained by putting the results of Lemmas A.1, A.5 and Propositions A.2 and A.3 together. \square

References

- [1] G.D. Birkhoff, Nouvelles Recherches sur les systèmes dynamiques, Mém. Pont. Acad. Sci. Novi Lyncae 1 (1935) 85–216, in particular, Chapter IV.
- [2] M. Benedicks, L. Carleson, The dynamics of the Hénon map, Ann. of Math. 133 (1991) 73–169.
- [3] R. Bowen, Periodic points and measures for Axiom A diffeomorphisms, Trans. Amer. Math. Soc. (1971) 377–397.
- [4] M. Benedicks, L.-S. Young, Sinai–Bowen–Ruelle measures for certain Hénon maps, Invent. Math. 112 (1993) 541–576.
- [5] M.L. Cartwright, J.E. Littlewood, On non-linear differential equations of the second order, I: The equation $\ddot{y} + k(1 - y^2)\dot{y} + y = b\lambda k \cos(\lambda t + a)$, k large, J. Lond. Math. Soc. 20 (1945) 180–189.
- [6] G. Duffing, Erzwungene Schwingungen bei Veränderlicher Eigenfrequenz, F. Wieweg u. Sohn, Braunschweig, 1918.
- [7] J. Guckenheimer, P. Holmes, Nonlinear Oscillations, Dynamical Systems and Bifurcation of Vector Fields, Appl. Math. Sci., vol. 42, Springer-Verlag, 1983.
- [8] M. Hénon, A two-dimensional mapping with a strange attractor, Comm. Math. Phys. 50 (1976) 69–77.
- [9] F. Ledrappier, Propriétés ergodiques des mesures de Sinai, Publ. Math. Inst. Hautes Etudes Sci. 59 (1984) 163–188.

- [10] M. Levi, Qualitative analysis of the periodically forced relaxation oscillators, *Mem. Amer. Math. Soc.* 214 (1981).
- [11] N. Levinson, A second-order differential equation with singular solutions, *Ann. of Math.* 50 (1949) 127–153.
- [12] E.N. Lorenz, Deterministic non-periodic flow, *J. Amer. Sci.* 20 (1963) 130–141.
- [13] V.K. Melnikov, On the stability of the center for time-periodic perturbations, *Trans. Moscow Math. Soc.* 12 (1963) 1–56.
- [14] J.K. Moser, *Stable and Random Motions in Dynamical Systems (with Special Emphasis on Celestial Mechanics)*, Princeton University Press, Princeton, NJ, 1973.
- [15] L. Mora, M. Viana, Abundance of strange attractors, *Acta Math.* 171 (1993) 1–71.
- [16] S.E. Newhouse, Diffeomorphisms with infinitely many sinks, *Topology* 13 (1974) 9–18.
- [17] J. Palis, F. Takens, *Hyperbolicity & Sensitive Chaotic Dynamics at Homoclinic Bifurcations*, Cambridge Stud. Adv. Math., vol. 35, Cambridge University Press, Cambridge, 1993.
- [18] H. Poincaré, *Les Méthodes Nouvelles de la Mécanique Céleste*, vols. 1–3, Gauthier-Villars, Paris, 1899.
- [19] Ja.B. Pesin, Characteristic Lyapunov exponents and smooth ergodic theory, *Russian Math. Surveys* 32.4 (1977) 55–114.
- [20] D. Ruelle, Ergodic theory of differentiable dynamical systems, *Publ. Math. Inst. Hautes Etudes Sci.* 50 (1979) 27–58.
- [21] Y.G. Sinai, Gibbs measure in ergodic theory, *Russian Math. Surveys* 27 (1972) 21–69.
- [22] S. Smale, Diffeomorphisms with many periodic points, in: *Differential and Combinatorial Topology (A Symposium in Honor of Marston Morse)*, Princeton University Press, 1965, pp. 68–80.
- [23] L.P. Shilnikov, On a Poincaré–Birkhoff problem, *Math. USSR-Sb.* 3 (1967) 353–371.
- [24] L.P. Shilnikov, A.L. Shilnikov, D. Turaev, L. Chua, *Methods of Qualitative Theory in Nonlinear Dynamics. Part I*, World Sci. Ser. Nonlinear Sci. Ser. A Monogr. Treatises, vol. 4, World Scientific Publishing Co., Inc., River Edge, NJ, 1998.
- [25] L.P. Shilnikov, A.L. Shilnikov, D. Turaev, L. Chua, *Methods of Qualitative Theory in Nonlinear Dynamics. Part II*, World Sci. Ser. Nonlinear Sci. Ser. A Monogr. Treatises, vol. 5, World Scientific Publishing Co., Inc., River Edge, NJ, 2001.
- [26] B. von de Pol, Forced oscillations in a circuit with non-linear resistance (receptance with reactive triode), *London, Edinburg and Dublin Phil. Mag.* 3 (1927) 65–80.
- [27] Q.D. Wang, A. Oksasoglu, On the dynamics of certain homoclinic tangles, *J. Differential Equations* 250 (2011) 710–751.
- [28] Q.D. Wang, A. Oksasoglu, Periodic occurrence of chaotic behavior of homoclinic tangles, *Physica D: Nonlinear Phenomena* 239 (7) (2010) 387–395.
- [29] Qiudong Wang, William Ott, Dissipative Homoclinic Loops of Two-Dimensional Maps and Strange Attractors with One Direction of Instability, *Comm. Pure Appl. Math.* 64 (11) (2011) 1439–1496.
- [30] Q.D. Wang, L.-S. Young, Strange attractors with one direction of instability, *Comm. Math. Phys.* 218 (2001) 1–97.
- [31] Q.D. Wang, L.-S. Young, Toward a theory of rank one attractors, *Ann. of Math.* 167 (2008) 349–480.
- [32] Q.D. Wang, L.-S. Young, From invariant curves to strange attractors, *Comm. Math. Phys.* 225 (2002) 275–304.
- [33] Q.D. Wang, L.-S. Young, Strange attractors in periodically-kicked limit cycles and Hopf bifurcations, *Comm. Math. Phys.* 240 (2003) 509–529.